ELSEVIER

International Journal of Solids and Structures 41 (2004) 4237–4260

INTERNATIONAL JOURNAL OF SOLIDS and STRUCTURES

www.elsevier.com/locate/ijsolstr

A transversely isotropic viscohyperelastic material Application to the modeling of biological soft connective tissues

Georges Limbert [a,b,*], John Middleton [a]

[a] *Biomechanics Research Unit, The Cardiff Medicentre, University of Wales College of Medicine, Cardiff, CF14 4UJ, UK*
[b] *FIRST Numerics Ltd, UK*

Received 27 January 2003; received in revised form 20 February 2004
Available online 27 March 2004

Abstract

A general transversely isotropic viscohyperelastic constitutive law including strain rate effects was proposed. It is based on a definition of a general Helmholtz free energy function which depends explicitly on the right Cauchy–Green deformation tensor, its material time derivative and a structural tensor characterizing the preferred direction from which anisotropy arises. The elastic and viscous potentials that defined the free energy function were assumed to be decoupled, thus facilitating the identification process. This law was valid for arbitrary kinematics and aimed at modeling the mechanical behavior of biological soft tissues at high strain rates and at the finite strain regime. This is of high relevance for dynamic analyses of human occupants in car crash simulations (finite element analyses) and for situations where dynamic loads are significant (sport injury, etc). Explicit expression of the stress, elasticity and viscosity tensors were established. As an application of the constitutive law, the general expressions of the stress tensors were particularized for a specific Helmholtz free energy function describing the mechanical characteristics of the human anterior cruciate ligament. The constitutive model was shown to capture the strain rate effects and other essential characteristics of ligaments such as finite strain, anisotropy and nearly incompressibility. The model was also tested for various multi-axial loading situations.

Keywords: Hyperelasticity; Transverse isotropy; Fiber-reinforced composite; Strain rate; Viscoelasticity; Biological soft tissue; ACL; Ligament; Biomechanics

1. Introduction

The main characteristics of biological soft connective tissues are that they sustain large deformations, rotations and displacements, have a highly non-linear behavior and possess strongly anisotropic mechanical

* Corresponding author. Address: Biomechanics Research Unit, Cardiff Medicentre, University of Wales College of Medicine, Cardiff, CF14 4UJ, UK. Tel.: +44-2920682162; fax: +44-29-2068-2161.
E-mail address: limbertg@cardiff.ac.uk (G. Limbert).
URL: http://www.firstnumerics.com.

0020-7683/$ - see front matter © 2004 Published by Elsevier Ltd.
doi:10.1016/j.ijsolstr.2004.02.057

properties (Fung, 1973). Moreover, their behavior is known to be viscoelastic, and this is especially relevant as the loading rates involved increase. It was shown that the shape of the stress–strain curves at which traction tests are performed is affected by the loading rate (Chiba and Komatsu, 1993; Haut, 1983; Kennedy et al., 1976; Nowalk and Logan, 1991; Pioletti et al., 1998; Ticker et al., 1996). The study of the influence of the strain rate on the stress–strain relations shows a general trend for an increase in stress with a corresponding increasing in the strain rate (Haut and Little, 1972). Although several three-dimensional continuum anisotropic viscohyperelastic models have been proposed in the past (Holzapfel, 2000; Puso and Weiss, 1998), their domain of validity is restricted to low strain rates (0.06–0.75 $\%\,s^{-1}$) (Haut and Little, 1972) and give inaccurate results for higher strain rates (up to 10 $\%\,s^{-1}$) (Woo et al., 1981).

The continuum constitutive framework developed by Pioletti et al. (1998) was advantageous in that it was able to encompass strain rate effects (short-term memory effects) by using the rate of deformation as an explicit variable. However, a serious shortcoming of the constitutive law was the assumption of isotropy. In fact, due to their fibrous structure (collagen fibers embedded in a highly compliant solid matrix), ligaments should be modeled as anisotropic structures for most physiological situations where states of pure tension along the fiber directions are rather the exception than the rule (Limbert, 2001; Limbert and Taylor, 2001a; Limbert and Taylor, 2001b; Limbert and Taylor, 2002).

The first objective of the present study is therefore to extend the work from Pioletti et al. (1998) to the transversely isotropic case (the simplest form of anisotropy) by combining the constitutive framework of Noll (1958) and the theory of continuum fiber-reinforced composite of Spencer (Limbert and Taylor, 2002; Spencer, 1992).

The second objective is to propose a simple example of application of the constitutive framework by proposing an original constitutive law and identifying the material parameters with experimental data for the human anterior cruciate ligament (ACL) (Pioletti et al., 1998).

2. Basic results in continuum mechanics

2.1. Kinematics

Following standard usage in continuum mechanics, we denote by $\mathbf{F}$, the gradient of the deformation $\varphi(\mathbf{X},t)$:

$$\mathbf{F}(\mathbf{X},t) := \frac{\partial \varphi(\mathbf{X},t)}{\partial \mathbf{X}} = \sum_{i,I=1}^{3} \frac{\partial \varphi_i}{\partial X_I} \mathbf{e}_i \otimes \mathbf{E}_I \tag{1}$$

$\mathbf{X}$ is the position of the material point in the reference configuration whilst t is the usual time parameter. $\{\mathbf{E}_I\}_{I=1,2,3}$ and $\{\mathbf{e}_i\}_{i=1,2,3}$ are fixed orthonormal bases in the Lagrangean and Eulerian configurations respectively. The uppercase and lowercase letters used in indicial notation refer to the reference and the deformed (current) configuration, respectively. The right and left Cauchy–Green deformation tensors are respectively defined as

$$\mathbf{C} := \mathbf{F}^{\mathrm{T}} \cdot \mathbf{F} \quad \text{and} \quad \mathbf{b} := \mathbf{F} \cdot \mathbf{F}^{\mathrm{T}} \tag{2}$$

where the superscript 'T' denotes the transpose of the linear transformation. For future developments, one also defines $\mathbf{1}$ as the second-order identity tensor. The rate of the deformation gradient, also called material velocity gradient, is given by

$$\dot{\mathbf{F}} = \dot{\mathbf{F}}(\mathbf{X},t) = \frac{\partial \mathbf{F}}{\partial t} = \frac{\partial^2 \mathbf{x}}{\partial \mathbf{X} \partial t} = \frac{\partial \dot{\mathbf{u}}}{\partial \mathbf{X}} = \mathbf{l} \cdot \mathbf{F} \tag{3}$$

where $\mathbf{l}$ is the spatial velocity gradient

$$\mathbf{l} = \dot{\mathbf{F}} \cdot \mathbf{F}^{-1} \tag{4}$$

The rate of the material metric tensor is an objective tensor expressed as follows:

$$\dot{\mathbf{C}} = \dot{\mathbf{C}}(\mathbf{X}, t) = \dot{\mathbf{F}}^{\mathrm{T}} \cdot \mathbf{F} + \mathbf{F}^{\mathrm{T}} \cdot \dot{\mathbf{F}} = 2\mathbf{F}^{\mathrm{T}} \cdot \mathbf{d} \cdot \mathbf{F} \tag{5}$$

where $\mathbf{d}$, the spatial rate of deformation tensor, is the symmetric part of $\mathbf{l}$

$$\mathbf{d} = \frac{1}{2}(\mathbf{l} + \mathbf{l}^{\mathrm{T}}) \tag{6}$$

2.2. Material symmetry

Extensive work has been done on the subject of material symmetry (Cohen and Wang, 1987; Coleman and Noll, 1964; Ericksen, 1978; Ericksen, 1979; Ericksen and Rivlin, 1954; Negahban and Wineman, 1989a; Negahban and Wineman, 1989b; Wineman and Pipkin, 1964; Zheng and Boehler, 1994).

Boehler (1978) demonstrated that any scalar-, vector-, and second-order tensor-valued functions of vectors and second-order tensors relative to any anisotropy characterized in terms of vectors and second-order tensors can be expressed as an isotropic function of the original tensor agencies and the structural tensors as additional agencies. This means that the Helmholtz free energy function of an anisotropic material can be expressed as an isotropic function of its classical three principal strain invariants (as in the isotropic case) plus invariants relating the right Cauchy–Green deformation tensor, its material rate and any combination of structural tensors characterizing the anisotropy. Material symmetries are characterized by symmetry groups that impose restrictions on the form of the strain energy function (Ogden, 1984). Any orthogonal transformation member of the symmetry group of the material will leave the strain energy function unchanged when applied to the material in the natural state (prior to deformation).

3. Fiber-reinforced continuum

To describe the constitutive behavior of biological soft connective tissue in the case of transversely isotropic material symmetry, we consider a material constructed from one family of fibers continuously distributed in a (highly) compliant solid isotropic matrix (Fig. 1). The result of the geometrical and mechanical interactions of the two constituents gives the material directional macroscopic properties (Spencer, 1992). The family of fibers is characterized by a unit vector $\mathbf{n}_0(\mathbf{X})$ defined in the reference configuration. This vector defines locally the preferred directions from which the anisotropy directly arises and then the fiber directions can vary within the material. The structural tensor $\mathbf{N}_0 = \mathbf{n}_0 \otimes \mathbf{n}_0$ has to be introduced. It reflects the local structural arrangement of the fibers and thus defines local directional properties of the composite material. It is noteworthy that, by construction, $\mathbf{N}_0$ is a symmetric second-order tensor.

3.1. Thermodynamic considerations

The existence of a Helmoltz free energy function ψ, isotropic function of its arguments, is postulated. The strain energy function ψ is only a function of $\mathbf{X}$, $\mathbf{C}$, $\mathbf{N}_0$ and other second-order tensorial thermodynamic variables $\mathbf{A}_k$ and is therefore written as $\psi = \psi(\mathbf{X}, \mathbf{C}, \mathbf{N}_0, \mathbf{A}_k)$.

The invariance requirement of the Helmholtz free energy function with respect to the material symmetry group is automatically satisfied because the arguments of the function are quantities associated with the reference configuration.

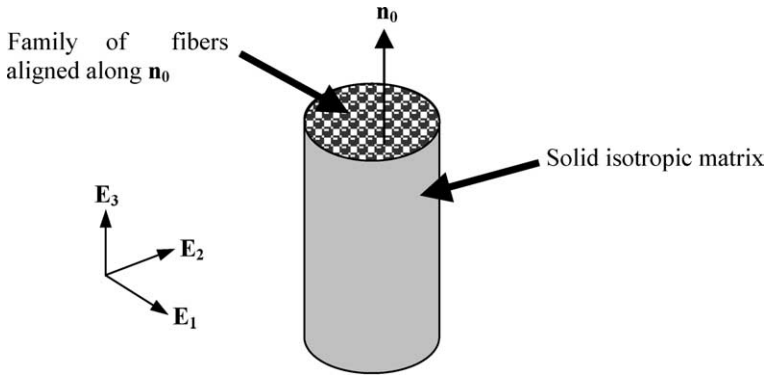

Fig. 1. Simplified representation of a continuum material made of an isotropic matrix reinforced by one familiy of fibers associated with direction $\mathbf{n}_0$ in the reference configuration. The particular arrangement of the fibers is defined locally and therefore depends on the position $\mathbf{X}$ of the material point. The set of unit vectors ($\mathbf{E}_1$, $\mathbf{E}_2$, $\mathbf{E}_3$) represent an orthonormal basis in the reference configuration.

In the subsequent developments, it is assumed that the thermomechanical phenomena involved operate at constant temperature (isothermal process). To formulate the constitutive equations attached to the proposed material model, it is firstly assumed that the equilibrium state of the viscoelastic solid at fixed $\mathbf{F}$ as $t \to \infty$ derives from a (hyperelastic) free energy function ψ^{e} (defined per unit reference volume)

$$\psi^{\mathrm{e}} = \psi^{\mathrm{e}}[\mathbf{X}, \mathbf{C}(\mathbf{X}), \mathbf{N}_0(\mathbf{X})] \tag{7}$$

This function is defined at any point $\mathbf{X}$ of the body and for any t of the time interval considered. For an isothermal process, the First and Second Principles of Thermodynamics reduce to the satisfaction of the Clausius–Duhem inequality (Truesdell and Noll, 1992)

$$\Xi_{\mathrm{int}} = \frac{1}{2}\mathbf{S} : \dot{\mathbf{C}} - \dot{\psi}^{\mathrm{e}} \geqslant 0 \tag{8}$$

where Ξ_{int} is the internal dissipation or local entropy production. By derivation of ψ with respect to time and combination with Eq. (8), we obtain

$$\Xi_{\mathrm{int}} = \frac{1}{2}\left(\mathbf{S} - 2\frac{\partial \psi^{\mathrm{e}}}{\partial \mathbf{C}}\right) : \dot{\mathbf{C}} \geqslant 0 \quad \forall\, \mathbf{C}, \dot{\mathbf{C}} \tag{9}$$

It is assumed that the local entropy is produced by viscous effects which derive from a viscous potential $\psi^{\mathrm{v}}[\mathbf{X}, \mathbf{C}(\mathbf{X}), \dot{\mathbf{C}}(\mathbf{X}), \mathbf{N}_0(\mathbf{X})]$. This leads us to write

$$\Xi_{\mathrm{int}} = \frac{\partial \psi^{\mathrm{v}}}{\partial \dot{\mathbf{C}}} : \dot{\mathbf{C}} = \frac{1}{2}\left(\mathbf{S} - 2\frac{\partial \psi}{\partial \dot{\mathbf{C}}}\right) : \dot{\mathbf{C}} \geqslant 0 \quad \forall\, \mathbf{C}, \dot{\mathbf{C}} \tag{10}$$

It is worthy to note that $\mathbf{C}$ is a parameter and not a variable in the definition of ψ^{v}. That means that coupling between elastic and viscous effects can be accounted for.

Following the standard Coleman–Noll procedure (Coleman and Gurtin, 1967; Coleman and Noll, 1963) to ensure that $\Xi_{\mathrm{int}} \geqslant 0$ for all admissible processes (arbitrary choices of $\dot{\mathbf{C}}$) the expression of the second Piola–Kirchhoff stress tensor is readily obtained as follows:

$$\mathbf{S} = \mathbf{S}^{\mathrm{e}} + \mathbf{S}^{\mathrm{v}} = 2\left(\frac{\partial \psi^{\mathrm{e}}}{\partial \mathbf{C}} + \frac{\partial \psi^{\mathrm{v}}}{\partial \dot{\mathbf{C}}}\right) \tag{11}$$

where the following expressions have been defined:

$$\mathbf{S}^{\mathrm{e}} = 2\frac{\partial \psi^{\mathrm{e}}}{\partial \mathbf{C}}, \quad \mathbf{S}^{\mathrm{v}} = 2\frac{\partial \psi^{\mathrm{v}}}{\partial \dot{\mathbf{C}}} \tag{12}$$

$\mathbf{S}^{\mathrm{e}}$ and $\mathbf{S}^{\mathrm{v}}$, the elastic and viscous second Piola–Kirchhoff stress tensors, represent the stress associated with, respectively, the equilibrium and non-equilibrium states in the Lagrangean configuration.

Finally, it is assumed the existence of a general thermodynamic potential ψ characterized by a split decomposition into an elastic and viscous potential ψ^{e} and ψ^{v}

$$\psi[\mathbf{X}, \mathbf{C}(\mathbf{X},t), \dot{\mathbf{C}}(\mathbf{X},t), \mathbf{N}_0(\mathbf{X})] = \psi^{\mathrm{e}}[\mathbf{X}, \mathbf{C}(\mathbf{X},t), \mathbf{N}_0(\mathbf{X})] + \psi^{\mathrm{v}}[\mathbf{X}, \mathbf{C}(\mathbf{X},t), \dot{\mathbf{C}}(\mathbf{X},t), \mathbf{N}_0(\mathbf{X})] \tag{13}$$

The additional tensorial thermodynamic variable $\mathbf{A}_k$ is identified with the deformation rate (symmetric) tensor $\dot{\mathbf{C}}$. For sake of clarity, the possible dependence on $\mathbf{X}$ and t of $\mathbf{C}$, $\dot{\mathbf{C}}$ and $\mathbf{N}_0$ will be omitted in the next developments. It is worthy to note that $\mathbf{C}$ is a parameter and not a variable in ψ^{v}.

A set of 17 invariants $\bar{I}_\alpha$ are necessary to form the *irreducible integrity bases* of the tensors $\mathbf{C}$, $\dot{\mathbf{C}}$ and $\mathbf{N}_0$ (Boehler, 1987). In other words, it must exist a strain energy function $\overline{\bar{\psi}}$, $\bar{\psi} : \{(\Re^+)\times\}^{17} \to \Re$ such that ψ can be written in the following form:

$$\psi(\mathbf{X}, \mathbf{C}, \dot{\mathbf{C}}, \mathbf{N}_0) = \overline{\bar{\psi}}[\{\bar{I}_\alpha(\mathbf{X}, \mathbf{C}, \dot{\mathbf{C}}, \mathbf{N}_0)\}_{\alpha=1\ldots17}] \tag{14}$$

The latest form of the strain energy function automatically satisfies the *principle of frame indifference* because it is defined from quantities associated with the reference state. To simplify the notations, ψ and $\overline{\bar{\psi}}$ are identified: $\psi(\mathbf{X}, \mathbf{C}, \dot{\mathbf{C}}, \mathbf{N}_0) = \psi[\mathbf{X}, \{I_\alpha(\mathbf{C}, \dot{\mathbf{C}}, \mathbf{N}_0)\}_{\alpha=1\ldots17}]$.

It is postulated that

$$\psi = \psi^{\mathrm{e}}[\{I_\alpha(\mathbf{X}, \mathbf{C}, \mathbf{N}_0)\}_{\alpha=1\ldots5}] + \psi^{\mathrm{v}}[\{J_\alpha(\mathbf{X}, \mathbf{C}, \dot{\mathbf{C}}, \mathbf{N}_0)\}_{\alpha=1\ldots12}] \tag{15}$$

The invariants defining ψ are the following:

$$I_1 = \mathbf{1} : \mathbf{C}, \quad I_2 = \frac{1}{2}[I_1^2 - (\mathbf{1} : \mathbf{C}^2)], \quad I_3 = \det(\mathbf{C}) \tag{16}$$

$$I_4 = \mathbf{N}_0 : \mathbf{C}, \quad I_5 = \mathbf{N}_0 : \mathbf{C}^2 \tag{17}$$

$$J_1 = \mathbf{1} : \dot{\mathbf{C}}, \quad J_2 = \frac{1}{2}(\mathbf{1} : \dot{\mathbf{C}}^2), \quad J_3 = \det(\dot{\mathbf{C}}) \tag{18}$$

$$J_4 = \mathbf{N}_0 : \dot{\mathbf{C}}, \quad J_5 = \mathbf{N}_0 : \dot{\mathbf{C}}^2 \tag{19}$$

$$J_6 = \mathbf{1} : (\mathbf{C} \cdot \dot{\mathbf{C}}), \quad J_7 = \mathbf{1} : (\mathbf{C} \cdot \dot{\mathbf{C}}^2), \quad J_8 = \mathbf{1} : (\mathbf{C}^2 \cdot \dot{\mathbf{C}}), \quad J_9 = \mathbf{1} : (\mathbf{C}^2\dot{\mathbf{C}}^2) \tag{20}$$

$$J_{10} = \mathbf{1} : (\mathbf{N}_0 \cdot \mathbf{C} \cdot \dot{\mathbf{C}}), \quad J_{11} = \mathbf{1} : (\mathbf{N}_0 \cdot \mathbf{C} \cdot \dot{\mathbf{C}}^2), \quad J_{12} = \mathbf{1} : (\mathbf{N}_0 \cdot \mathbf{C}^2 \cdot \dot{\mathbf{C}}) \tag{21}$$

The invariants I_1, I_2, I_3, J_1, J_2, J_3, J_6, J_7, J_8 and J_9 characterize the isotropic response of the material while the other complementary invariants are related to the transversely isotropic mechanical response of the material.

Observing that:

$$I_4 = \mathbf{n}_0 \cdot (\mathbf{C} \cdot \mathbf{n}_0) = (\lambda_{\mathbf{n}_0})^2 \tag{22}$$

where $\lambda_{\mathbf{n}_0}$ denotes the stretch associated with the direction $\mathbf{n}_0$, allows an easy physical interpretation of the invariants I_4 as shown in Eq. (22).

Upon deformation, the unit vector $\mathbf{n}_0$ (from the reference configuration) was transformed into a vector $\lambda_{\mathbf{n}_0}\mathbf{n}$ (Eq. (23)) where $\mathbf{n}$ represents the unit vector associated the single family of fibers in the distorted configuration

$$\lambda_{\mathbf{n}_0}\mathbf{n} = \sqrt{I_4}\mathbf{n} = \mathbf{F}\cdot\mathbf{n}_0 \tag{23}$$

3.2. Definition of stress tensors

Following Eqs. (11) and (15), the expression of the second Piola–Kirchhoff stress tensor is obtained as:

$$\mathbf{S} = 2\left[\sum_{\alpha=1}^{5}\left(\frac{\partial\psi^{\mathrm{e}}}{\partial I_\alpha}\frac{\partial I_\alpha}{\partial\mathbf{C}}\right) + \sum_{\alpha=1}^{12}\left(\frac{\partial\psi^{\mathrm{v}}}{\partial J_\alpha}\frac{\partial J_\alpha}{\partial\dot{\mathbf{C}}}\right)\right] \tag{24}$$

The elastic and viscous second Piola–Kirchhoff stress tensors are therefore

$$\mathbf{S}^{\mathrm{e}} = 2\sum_{\alpha=1}^{5}\left(\frac{\partial\psi^{\mathrm{e}}}{\partial I_\alpha}\frac{\partial I_\alpha}{\partial\mathbf{C}}\right) \tag{25}$$

$$\mathbf{S}^{\mathrm{v}} = 2\sum_{\alpha=1}^{12}\left(\frac{\partial\psi^{\mathrm{v}}}{\partial J_\alpha}\frac{\partial J_\alpha}{\partial\dot{\mathbf{C}}}\right) \tag{26}$$

The first derivatives of the 17 tensorial invariants with respect to $\mathbf{C}$ and $\dot{\mathbf{C}}$ are

$$\frac{\partial I_1}{\partial\mathbf{C}} = \mathbf{1},\quad \frac{\partial I_2}{\partial\mathbf{C}} = I_1\mathbf{1} - \mathbf{C},\quad \frac{\partial I_3}{\partial\mathbf{C}} = I_2\mathbf{1} - I_1\mathbf{C} + \mathbf{C}^2 = I_3\mathbf{C}^{-1} \tag{27}$$

$$\frac{\partial I_4}{\partial\mathbf{C}} = \mathbf{N}_0,\quad \frac{\partial I_5}{\partial\mathbf{C}} = \mathbf{n_0}\otimes\mathbf{C}\cdot\mathbf{n}_0 + \mathbf{n}_0\cdot\mathbf{C}\otimes\mathbf{n}_0 := \boldsymbol{\Upsilon}_{\mathbf{n}_0\mathbf{C}} \tag{28}$$

$$\frac{\partial J_1}{\partial\dot{\mathbf{C}}} = \mathbf{1},\quad \frac{\partial J_2}{\partial\dot{\mathbf{C}}} = \dot{\mathbf{C}},\quad \frac{\partial J_3}{\partial\dot{\mathbf{C}}} = J_2\mathbf{1} - J_1\dot{\mathbf{C}} + \dot{\mathbf{C}}^2 = J_3\dot{\mathbf{C}}^{-1} \tag{29}$$

$$\frac{\partial J_4}{\partial\dot{\mathbf{C}}} = \mathbf{N}_0,\quad \frac{\partial J_5}{\partial\dot{\mathbf{C}}} = \mathbf{n}_0\otimes\dot{\mathbf{C}}\cdot\mathbf{n}_0 + \mathbf{n}_0.\dot{\mathbf{C}}\otimes\mathbf{n}_0 := \boldsymbol{\Upsilon}_{\mathbf{n}_0\dot{\mathbf{C}}} \tag{30}$$

$$\frac{\partial J_6}{\partial\dot{\mathbf{C}}} = \mathbf{C},\quad \frac{\partial J_7}{\partial\dot{\mathbf{C}}} = \mathbf{C}\cdot\dot{\mathbf{C}} + \dot{\mathbf{C}}\cdot\mathbf{C},\quad \frac{\partial J_8}{\partial\dot{\mathbf{C}}} = \mathbf{C}^2,\quad \frac{\partial J_9}{\partial\dot{\mathbf{C}}} = \mathbf{C}^2\cdot\dot{\mathbf{C}} + \dot{\mathbf{C}}\cdot\mathbf{C}^2 \tag{31}$$

$$\frac{\partial J_{10}}{\partial\dot{\mathbf{C}}} = \mathbf{N}_0\cdot\mathbf{C},\quad \frac{\partial J_{11}}{\partial\dot{\mathbf{C}}} = \mathbf{N}_0\cdot\mathbf{C}\cdot\dot{\mathbf{C}} + \dot{\mathbf{C}}\cdot\mathbf{N}_0\cdot\mathbf{C},\quad \frac{\partial J_{12}}{\partial\dot{\mathbf{C}}} = \mathbf{N}_0\cdot\mathbf{C}^2 \tag{32}$$

After algebraic manipulations, the expression of $\mathbf{S}^{\mathrm{e}}$ and $\mathbf{S}^{\mathrm{v}}$ are obtained as

$$\mathbf{S}^{\mathrm{e}} = 2[(\psi_1^{\mathrm{e}} + I_1\psi_2^{\mathrm{e}})\mathbf{1} - \psi_2^{\mathrm{e}}\mathbf{C} + I_3\psi_3^{\mathrm{e}}\mathbf{C}^{-1} + \psi_4^{\mathrm{e}}\mathbf{N}_0 + \psi_5^{\mathrm{e}}\boldsymbol{\Upsilon}_{\mathbf{n}_0\mathbf{C}}] \tag{33}$$

$$\begin{aligned}\mathbf{S}^{\mathrm{v}}c = {} & +2[\psi_1^{\mathrm{v}}\mathbf{1} + \psi_2^{\mathrm{v}}\dot{\mathbf{C}} + J_3\psi_3^{\mathrm{v}}\dot{\mathbf{C}}^{-1} + \psi_4^{\mathrm{v}}\mathbf{N}_0 + \psi_5^{\mathrm{v}}\boldsymbol{\Upsilon}_{\mathbf{n}_0\dot{\mathbf{C}}}]\\ & + 2[\psi_6^{\mathrm{v}}\mathbf{C} + \psi_7^{\mathrm{v}}(\mathbf{C}\cdot\dot{\mathbf{C}} + \dot{\mathbf{C}}\cdot\mathbf{C}) + \psi_8^{\mathrm{v}}\mathbf{C}^2 + \psi_9^{\mathrm{v}}(\mathbf{C}^2\cdot\dot{\mathbf{C}} + \dot{\mathbf{C}}\cdot\mathbf{C}^2)]\\ & + 2[\psi_{10}^{\mathrm{v}}(\mathbf{N}_0\cdot\mathbf{C}) + \psi_{11}^{\mathrm{v}}(\mathbf{N}_0\cdot\mathbf{C}\cdot\dot{\mathbf{C}} + \dot{\mathbf{C}}\cdot\mathbf{N}_0\cdot\mathbf{C}) + \psi_{12}^{\mathrm{v}}(\mathbf{N}_0\cdot\mathbf{C}^2)]\end{aligned} \tag{34}$$

where the following notations $\psi_\alpha^{\mathrm{e}} = \frac{\partial\psi^{\mathrm{e}}}{\partial I_\alpha}$ and $\psi_\alpha^{\mathrm{v}} = \frac{\partial\psi^{\mathrm{v}}}{\partial J_\alpha}$ have been introduced.

In finite elasticity, the Cauchy stress tensor is typically calculated from the second Piola–Kirchhoff stress tensor by means of the *push-forward* operation φ_* (Marsden and Hughes, 1994):

$$\boldsymbol{\sigma} = \boldsymbol{\sigma}^{\mathrm{e}} + \boldsymbol{\sigma}^{\mathrm{v}} = \frac{1}{J}(\varphi_* \mathbf{S}) \tag{35}$$

where

$$\boldsymbol{\sigma}^{\mathrm{e}} = \frac{1}{J}(\varphi_* \mathbf{S}^{\mathrm{e}}) = \frac{1}{J}\mathbf{F}\cdot\mathbf{S}^{\mathrm{e}}\cdot\mathbf{F}^{\mathrm{T}} = \frac{2}{J}\mathbf{F}\cdot\left(\frac{\partial\psi^{\mathrm{e}}}{\partial\mathbf{C}}\right)\cdot\mathbf{F}^{\mathrm{T}} \tag{36}$$

$$\boldsymbol{\sigma}^{\mathrm{v}} = \frac{1}{J}(\varphi_* \mathbf{S}^{\mathrm{v}}) = \frac{1}{J}\mathbf{F}\cdot\mathbf{S}^{\mathrm{v}}\cdot\mathbf{F}^{\mathrm{T}} = \frac{2}{J}\mathbf{F}\cdot\left(\frac{\partial\psi^{\mathrm{v}}}{\partial\dot{\mathbf{C}}}\right)\cdot\mathbf{F}^{\mathbf{T}} \tag{37}$$

This leads to the following forms for the elastic and viscous Cauchy stress tensors:

$$\boldsymbol{\sigma}^{\mathrm{e}} = \frac{2}{J}[(\psi_1^{\mathrm{e}} + I_1\psi_2^{\mathrm{e}})\mathbf{b} - \psi_2^{\mathrm{e}}\mathbf{b}^2 + I_3\psi_3^{\mathrm{e}}\mathbf{1} + I_4\psi_4^{\mathrm{e}}\mathbf{N} + I_4\psi_5^{\mathrm{e}}\boldsymbol{\Upsilon}_{\mathbf{nb}}] \tag{38}$$

$$\begin{aligned}\boldsymbol{\sigma}^{\mathrm{v}} = {} & \frac{2}{J}[\psi_1^{\mathrm{v}}\mathbf{b} + 2\psi_2^{\mathrm{v}}\mathbf{b}\cdot(\mathbf{b}\cdot\mathbf{d} + \mathbf{d}\cdot\mathbf{b})\cdot\mathbf{b} + J_3\psi_3^{\mathrm{v}}(\mathbf{l}^{-1} + \mathbf{l}^{-\mathrm{T}}) + I_4\psi_4^{\mathrm{v}}\mathbf{N} + 2I_4\psi_5^{\mathrm{v}}\boldsymbol{\Upsilon}_{\mathbf{nbd}}] \\ & + \frac{2}{J}[\psi_6^{\mathrm{v}}\mathbf{b}^2 + 2\psi_7^{\mathrm{v}}(\mathbf{b}^3\cdot\mathbf{d}\cdot\mathbf{b} + \mathbf{b}\cdot\mathbf{d}\cdot\mathbf{b}^3) + \psi_8^{\mathrm{v}}\mathbf{b}^3 + 2\psi_9^{\mathrm{v}}\mathbf{b}\cdot(\mathbf{b}^2\cdot\mathbf{d} + \mathbf{d}\cdot\mathbf{b}^2)\cdot\mathbf{b}] \\ & + \frac{2}{J}[\psi_{10}^{\mathrm{v}}I_4(\mathbf{N}\cdot\mathbf{b}) + 2I_4\psi_{11}^{\mathrm{v}}(\mathbf{N}\cdot\mathbf{b}\cdot\mathbf{d}\cdot\mathbf{b} + \mathbf{b}\cdot\mathbf{d}\cdot\mathbf{N}\cdot\mathbf{b}) + I_4\psi_{12}^{\mathrm{v}}(\mathbf{N}\cdot\mathbf{b}^2)]\end{aligned} \tag{39}$$

where the following notations have been introduced:

$$\mathbf{N} := \mathbf{n}\otimes\mathbf{n} \tag{40}$$

$$\boldsymbol{\Upsilon}_{\mathbf{nb}} := \mathbf{n}\otimes\mathbf{b}\cdot\mathbf{n} + \mathbf{n}\cdot\mathbf{b}\otimes\mathbf{n} \tag{41}$$

$$\boldsymbol{\Upsilon}_{\mathbf{nbd}} := \mathbf{n}\otimes\mathbf{b}\cdot\mathbf{d}\cdot\mathbf{b}\cdot\mathbf{n} + \mathbf{n}\cdot\mathbf{b}\cdot\mathbf{d}\cdot\mathbf{b}\otimes\mathbf{n} \tag{42}$$

To the best of our knowledge, these closed-form expressions of the viscous stress tensors, in the material and spatial configurations, appear to have not been previously reported in the literature.

3.3. Definition of the elasticity and viscous tensors

In this section, the expressions of the elasticity and viscosity tensors in the material configurations are derived. Not only do these tensors specify the response of the material to applied strain and strain rate, but they also give criteria about the actual stability of the structure. However, the discussion of the later concept is out of the scope of this work. These tensors will also prove to be essential for any finite element implementation of the material model.

3.3.1. Elasticity and viscosity tensors in the material configuration

Given the structure of the proposed Helmholtz free energy function ψ, the material elasticity and viscous tensors are defined through the following split form:

$$\mathbf{S} = \mathbf{A}_{m}^{\mathrm{e}} : \mathbf{C} + \mathbf{A}_{m}^{\mathrm{v}} : \dot{\mathbf{C}} \tag{43}$$

where

$$\mathbf{A}^{\mathrm{e}}_{\mathscr{m}} = 4\frac{\partial^2\psi^{\mathrm{e}}}{\partial\mathbf{C}\partial\mathbf{C}} = 2\frac{\partial\mathbf{S}^{\mathrm{e}}}{\partial\mathbf{C}} = 2\frac{\partial S^{\mathrm{e}}_{IJ}}{\partial C_{KL}}\mathbf{E}_I\otimes\mathbf{E}_J\otimes\mathbf{E}_K\otimes\mathbf{E}_L \tag{44}$$

$$\mathbf{A}^{\mathrm{v}}_{\mathscr{m}} = 4\frac{\partial^2\psi^{\mathrm{v}}}{\partial\dot{\mathbf{C}}\partial\dot{\mathbf{C}}} = 2\frac{\partial\mathbf{S}^{\mathrm{v}}}{\partial\dot{\mathbf{C}}} = 2\frac{\partial S^{\mathrm{v}}_{IJ}}{\partial\dot{C}_{KL}}\mathbf{E}_I\otimes\mathbf{E}_J\otimes\mathbf{E}_K\otimes\mathbf{E}_L \tag{45}$$

The elasticity tensors thus defined possesses the so-called *minor* and *major symmetries* which can be expressed in indicial notation

$$(\mathbf{A}^{\mathrm{e,v}}_{\mathscr{m}})_{IJKL} = (\mathbf{A}^{\mathrm{e,v}}_{\mathscr{m}})_{KLIJ} = (\mathbf{A}^{\mathrm{e,v}}_{\mathscr{m}})_{IJLK} = (\mathbf{A}^{\mathrm{e,v}}_{\mathscr{m}})_{JILK} \tag{46}$$

In order to obtain a convenient form for $\mathbf{A}^{\mathscr{m}}$, we introduce the following notations (Marsden and Hughes, 1994):

$$(\mathbf{I})_{IJKL} := \frac{\partial C_{IJ}}{\partial C_{KL}} = \frac{1}{2}(\delta_{IK}\delta_{JL} + \delta_{IL}\delta_{JK}) \tag{47}$$

$$(\mathbf{I}^{-1}_{\mathbf{C}})_{IJKL} := \frac{\partial C^{-1}_{IJ}}{\partial C_{KL}} = -\frac{1}{2}(C^{-1}_{IK}C^{-1}_{JL} + C^{-1}_{IL}C^{-1}_{JK}) \tag{48}$$

$$(\mathbf{I}^{-1}_{\dot{\mathbf{C}}})_{IJKL} := \frac{\partial \dot{C}^{-1}_{IJ}}{\partial \dot{C}_{KL}} = -\frac{1}{2}(\dot{C}^{-1}_{IK}\dot{C}^{-1}_{JL} + \dot{C}^{-1}_{IL}\dot{C}^{-1}_{JK}) \tag{49}$$

$\mathbf{I}$ is the identity mapping on the six-dimensional space of symmetric second-order tensors and $\boldsymbol{\delta}$ is the Kronecker tensor ($\delta_{IJ} = 1$ if $I = J$, 0 otherwise).

In order to condense the next developments, the following notations are introduced: $\psi^{\mathrm{e}}_{\alpha\beta} = \frac{\partial\psi^{\mathrm{e}}}{\partial I_\alpha\partial I_\beta}$, $\psi^{\mathrm{v}}_{\alpha\beta} = \frac{\partial\psi^{\mathrm{v}}}{\partial J_\alpha\partial J_\beta}$, $\Delta^{\mathrm{v}}_\alpha := \frac{\partial\psi^{\mathrm{v}}_\alpha}{\partial\dot{\mathbf{C}}}$, $_{\alpha=1\ldots12}$, where the expression of $\Delta^{\mathrm{v}}_\alpha$ is given below

$$\begin{aligned}\Delta^{\mathrm{v}}_\alpha := \frac{\partial\psi^{\mathrm{v}}_\alpha}{\partial\dot{\mathbf{C}}} &= \frac{\partial^2\psi^{\mathrm{v}}}{\partial J_1\partial J_\alpha}\mathbf{1} + \frac{\partial^2\psi^{\mathrm{v}}}{\partial J_2\partial J_\alpha}\dot{\mathbf{C}} + \frac{\partial^2\psi^{\mathrm{v}}}{\partial J_3\partial J_\alpha}\dot{\mathbf{C}}^2 + \frac{\partial^2\psi^{\mathrm{v}}}{\partial J_4\partial J_\alpha}\mathbf{N}_0 + \frac{\partial^2\psi^{\mathrm{v}}}{\partial J_5\partial J_\alpha}\boldsymbol{\Upsilon}_{\mathbf{n}_0\dot{\mathbf{C}}}\\ &+ \frac{\partial^2\psi^{\mathrm{v}}}{\partial J_6\partial J_\alpha}\mathbf{C} + \frac{\partial^2\psi^{\mathrm{v}}}{\partial J_7\partial J_\alpha}\left(\mathbf{C}\cdot\dot{\mathbf{C}} + \dot{\mathbf{C}}\cdot\mathbf{C}\right) + \frac{\partial^2\psi^{\mathrm{v}}}{\partial J_8\partial J_\alpha}\mathbf{C}^2 + \frac{\partial^2\psi^{\mathrm{v}}}{\partial J_9\partial J_\alpha}(\mathbf{C}^2\cdot\dot{\mathbf{C}} + \dot{\mathbf{C}}\cdot\mathbf{C}^2)\\ &+ \frac{\partial^2\psi^{\mathrm{v}}}{\partial J_{10}\partial J_\alpha}\mathbf{N}_0\cdot\mathbf{C} + \frac{\partial^2\psi^{\mathrm{v}}}{\partial J_{11}\partial J_\alpha}(\mathbf{N}_0\cdot\mathbf{C}\cdot\dot{\mathbf{C}} + \dot{\mathbf{C}}\cdot\mathbf{N}_0\cdot\mathbf{C}) + \frac{\partial^2\psi^{\mathrm{v}}}{\partial J_{12}\partial J_\alpha}\mathbf{N}_0\cdot\mathbf{C}^2\end{aligned} \tag{50}$$

Differentiating Eq. (33) with respect to $\mathbf{C}$ leads to the following form for $\mathbf{A}^{\mathrm{e}}_{\mathscr{m}}$:

$$\begin{aligned}\mathbf{A}^{\mathrm{e}}_{\mathscr{m}} &= 4[(\psi^{\mathrm{e}}_{11} + 2I_1\psi^{\mathrm{e}}_{12} + \psi^{\mathrm{e}}_2 + I_1^2\psi^{\mathrm{e}}_{22})\mathbf{1}\otimes\mathbf{1} - (\psi^{\mathrm{e}}_{12} + I_1\psi^{\mathrm{e}}_{22})(\mathbf{1}\otimes\mathbf{C} + \mathbf{C}\otimes\mathbf{1}) + \psi^{\mathrm{e}}_{22}(\mathbf{C}\otimes\mathbf{C}) - \psi^{\mathrm{e}}_2\mathbf{I}]\\ &+ 4[(I_3\psi^{\mathrm{e}}_3 + I_3^2\psi^{\mathrm{e}}_{33})\mathbf{C}^{-1}\otimes\mathbf{C}^{-1} + I_3\psi^{\mathrm{e}}_3\mathbf{I}^{-1}_{\mathbf{C}} + I_3(\psi^{\mathrm{e}}_{13} + I_1\psi^{\mathrm{e}}_{23})(\mathbf{1}\otimes\mathbf{C}^{-1} + \mathbf{C}^{-1}\otimes\mathbf{1})]\\ &+ 4[-I_3\psi^{\mathrm{e}}_{23}(\mathbf{C}\otimes\mathbf{C}^{-1} + \mathbf{C}^{-1}\otimes\mathbf{C})] + 4[(\psi^{\mathrm{e}}_{14} + I_1\psi^{\mathrm{e}}_{24} + \psi^{\mathrm{e}}_5)(\mathbf{1}\otimes\mathbf{N}_0 + \mathbf{N}_0\otimes\mathbf{1})\\ &+ (\psi^{\mathrm{e}}_{15} + I_1\psi^{\mathrm{e}}_{25})(\mathbf{1}\otimes\mathbf{N}_{0\mathrm{C}} + \mathbf{N}_{0\mathrm{C}}\otimes\mathbf{1})] + 4[-\psi^{\mathrm{e}}_{24}(\mathbf{C}\otimes\mathbf{N}_0 + \mathbf{N}_0\otimes\mathbf{C}) - \psi^{\mathrm{e}}_{25}(\mathbf{C}\otimes\mathbf{N}_{0\mathrm{C}} + \mathbf{N}_{0\mathrm{C}}\otimes\mathbf{C})]\\ &+ 4[\psi^{\mathrm{e}}_{44}(\mathbf{N}_0\otimes\mathbf{N}_0) + \psi^{\mathrm{e}}_{45}(\mathbf{N}_0\otimes\mathbf{N}_{0\mathrm{C}} + \mathbf{N}_{0\mathrm{C}}\otimes\mathbf{N}_0) + \psi^{\mathrm{e}}_{55}\mathbf{N}_{0\mathrm{C}}\otimes\mathbf{N}_{0\mathrm{C}}]\\ &+ 4[I_3\psi^{\mathrm{e}}_{43}(\mathbf{C}^{-1}\otimes\mathbf{N}_0 + \mathbf{N}_0\otimes\mathbf{C}^{-1}) + I_3\psi^{\mathrm{e}}_{53}(\mathbf{C}^{-1}\otimes\mathbf{N}_{0\mathrm{C}} + \mathbf{N}_{0\mathrm{C}}\otimes\mathbf{C}^{-1})]\end{aligned} \tag{51}$$

Differentiating Eq. (34) with respect to $\dot{\mathbf{C}}$ leads to the following expression form for $\mathbf{A}^{\mathrm{v}}_{\mathscr{m}}$:

$$\begin{aligned}\mathbf{A}^{\mathrm{v}}_{\mathscr{m}} = &+4[\mathbf{1}\otimes\Delta^{\mathrm{v}}_1+\dot{\mathbf{C}}\otimes\Delta^{\mathrm{v}}_2+\psi^{\mathrm{v}}_2\mathbf{I}+\dot{\mathbf{C}}^2\otimes\Delta^{\mathrm{v}}_3+\psi^{\mathrm{v}}_3\mathbf{I}^{-1}_{\dot{\mathbf{C}}}]+4\Bigg[\mathbf{N}_0\otimes\Delta^{\mathrm{v}}_4+\boldsymbol{\Upsilon}_{\mathbf{n}_0\dot{\mathbf{C}}}\otimes\Delta^{\mathrm{v}}_5\\ &+\psi^{\mathrm{v}}_5\left(\mathbf{1}\otimes\frac{\partial\boldsymbol{\Upsilon}_{\mathbf{n}_0\dot{\mathbf{C}}}}{\partial\dot{\mathbf{C}}}+\frac{\partial\boldsymbol{\Upsilon}_{\mathbf{n}_0\dot{\mathbf{C}}}}{\partial\dot{\mathbf{C}}}\otimes\mathbf{1}\right)\Bigg]+4[\mathbf{C}\otimes\Delta^{\mathrm{v}}_6+(\mathbf{C}\cdot\dot{\mathbf{C}}+\dot{\mathbf{C}}\cdot\mathbf{C})\otimes\Delta^{\mathrm{v}}_7+2\psi^{\mathrm{v}}_7(\mathbf{1}\otimes\mathbf{C}+\mathbf{C}\otimes\mathbf{1})]\\ &+4[\mathbf{C}^2\otimes\Delta^{\mathrm{v}}_8+(\mathbf{C}^2\cdot\dot{\mathbf{C}}+\dot{\mathbf{C}}\cdot\mathbf{C}^2)\otimes\Delta^{\mathrm{v}}_9+\psi^{\mathrm{v}}_9(\mathbf{1}\otimes\mathbf{C}^2+\mathbf{C}^2\otimes\mathbf{1})]+4[(\mathbf{N}_0\cdot\mathbf{C})\otimes\Delta^{\mathrm{v}}_{10}\\ &+(\mathbf{N}_0\cdot\mathbf{C}\cdot\dot{\mathbf{C}}+\dot{\mathbf{C}}\cdot\mathbf{N}_0\cdot\mathbf{C})\otimes\Delta^{\mathrm{v}}_{11}+\psi^{\mathrm{v}}_{11}(\mathbf{1}\otimes\mathbf{N}_0\cdot\mathbf{C}+\mathbf{N}_0\cdot\mathbf{C}\otimes\mathbf{1})]+4[(\mathbf{N}_0\cdot\mathbf{C}^2)\otimes\Delta^{\mathrm{v}}_{12}]\end{aligned}\tag{52}$$

To the best of our knowledge, the expression of the viscosity tensor, containing coupling contributions between the matrix and the fibers, has been not previously reported in the literature. The explicit expression of the elasticity tensor, containing all possible coupling contributions between the matrix and the fibers, has been previously established by Almeida and Spilker (1998) and Limbert and Taylor (2002) while the explicit expression of the elasticity tensor for the incompressible case was first established by Weiss et al. (1996).

3.3.2. Elongation moduli in the material description

From the expression of the elasticity tensors one can define elongation moduli $\kappa^{\mathrm{e}}_{\mathbf{n}_0}$ (elastic response) and $\kappa^{\mathrm{v}}_{\mathbf{n}_0}$ (viscous response) associated with the fiber direction $\mathbf{n}_0$. They characterize the stress response associated with the deformation and deformation rate in the fiber directions and are therefore directly related to the appropriate structural tensors by the following relationships:

$$\kappa^{\mathrm{e}}_{\mathbf{n}_0}=\mathbf{N}_0:(\mathbf{A}^{\mathrm{e}}_{\mathscr{m}}\cdot\mathbf{N}_0)\tag{53}$$

$$\kappa^{\mathrm{v}}_{\mathbf{n}_0}=\mathbf{N}_0:(\mathbf{A}^{\mathrm{v}}_{\mathscr{m}}\cdot\mathbf{N}_0)\tag{54}$$

3.3.3. Bulk modulus in the material description

Similarly to elongation moduli, elastic and viscous bulk moduli can be respectively defined as follows:

$$\kappa^{\mathrm{e}}=\frac{1}{9}\mathbf{1}:(\mathbf{A}^{\mathrm{e}}_{\mathscr{m}}\cdot\mathbf{1})\tag{55}$$

$$\kappa^{\mathrm{v}}=\frac{1}{9}\mathbf{1}:(\mathbf{A}^{\mathrm{v}}_{\mathscr{m}}\cdot\mathbf{1})\tag{56}$$

The elastic bulk modulus characterizes the volumetric stresses associated with volumetric deformations of the material while the viscous bulk modulus is related to the volumetric stresses associated with spherical rates of deformation.

3.4. Elasticity and viscous tensor in the spatial configuration

The spatial counterpart of the material elasticity and viscous tensor, $\mathbf{A}^{\mathrm{e}}_{\mathscr{s}}$ and $\mathbf{A}^{\mathrm{v}}_{\mathscr{s}}$, are, respectively, defined by the push-forward relations:

$$(\mathbf{A}^{\mathrm{e}}_{\mathscr{s}})_{ijkl}=\frac{1}{J}F_{iI}F_{jJ}F_{kK}F_{lL}(\mathbf{A}^{\mathrm{e}}_{\mathscr{m}})_{IJKL}\tag{57}$$

$$(\mathbf{A}^{\mathrm{v}}_{\mathscr{s}})_{ijkl}=\frac{1}{J}F_{iI}F_{jJ}F_{kK}F_{lL}(\mathbf{A}^{\mathrm{v}}_{\mathscr{M}})_{IJKL}\tag{58}$$

4. A particular Helmholtz free energy function for biological soft connective tissues: modeling of the anterior cruciate ligament

Further to the previous theoretical developments and to define an anisotropic viscohyperelastic constitutive law, the existence of a Helmholtz free energy density ψ, isotropic function of its arguments $(I_1, I_3, I_4, J_2, J_5)$, is postulated. The choice of the specific invariants will be justified below. It is further hypothesized that this energy function can be represented by the sum of a strain energy function $\psi^{e}(I_1, I_3, I_4)$ and a viscous energy function $\psi^{v}(J_2, J_5)$:

$$\psi(I_1, I_3, I_4, J_2, J_5) = \psi^{e}(I_1, I_3, I_4) + \psi^{v}(J_2, J_5) \tag{59}$$

This particular hypothesis implies that elastic and viscous stresses are additive as hypothesized in numerous studies like that of Pioletti et al. (1998). However, it does not exclude the coupling between elastic and viscous invariants in the function $\psi^{v}(J_2, J_5)$ because the elastic invariants can be parameters $\psi^{v}(J_2, J_5)$. Based on these observations $\psi^{v}(J_2, J_5)$ is rewritten as $\psi^{v}(J_2, J_5, I_1, I_4)$. The additive decomposition of stress corresponds to a Kelvin–Voigt rheological model in which a spring and a dashpot are arranged in parallel.

Superposition principles are often used in biomechanics because of the complexity of the structures involved that means difficulty of experimental characterization of these interactions, and because it is very difficult to assume any particular coupling relations between various physical quantities—in our study: *elastic* and *viscous* potentials. One way of dealing with this problem is to assume a particular form (in our study elastic and viscous energies are additive), check how it performs in specific conditions and then compare the results with available experimental data. If the mathematical and experimental models are in good agreement then the initial assumption was valid. However, it is essential to keep in mind that the assumption is valid only for the particular conditions enforced. If the model is capable of predicting other loading situations which are not those used for the calibration of the material model, the validity of the model moves a step further.

4.1. Choice of the invariants characterizing the Helmholtz free energy function ψ

As I_1 is the sum of the square of the eigenvalues of the deformation gradient, it is a convenient invariant representing the multi-axial state of deformation within the material (see Eq. (16)-1), specifically the ground substance. I_4 is the square of the stretch in the fiber direction (see Eq. (22)) and has a therefore a straightforward physical interpretation which characterize the directional mechanical properties of the soft connective tissue introduced by the presence of collagen fibers. I_3 characterizes the volumetric response of the material (see Eq. (16)) and is directly related to the degree of compressibility.

The invariant J_2 is the sum of the square of the eigenvalues of the rate of deformation $\dot{\mathbf{C}}$ and is such that its derivative with respect to the rate of the right Cauchy–Green deformation tensor is the rate itself (see Eq. (29)-2). This ensures that a viscous energy function of J_2 (first-order term) will lead to terms in the viscous stress response that are linearly dependent on the rate of deformation $\dot{\mathbf{C}}$.

It is noteworthy that, in these conditions, the viscous response does not include non-linear terms in $\dot{\mathbf{C}}$. This can be a limiting hypothesis that needs further investigation. In fact, failure to include non-linear terms may lead to a constitutive model that does not capture specific non-linear effects. However, in this particular case it will be shown (Fig. 2 and Table 2) that a linear term (in $\dot{\mathbf{C}}$) captures well the viscohyperelastic mechanical response of the ACL.

J_5 was chosen as the second invariant to characterize the anisotropic response of the viscous potential ψ^{v}. In a similar manner as J_2, J_5 represent the sum of the square of the eigenvalues of the rate of deformation $\dot{\mathbf{C}}$ projected along the fiber direction. The derivative of J_5 with respect to $\dot{\mathbf{C}}$ leads to a viscous stress term depending explicitly on $\dot{\mathbf{C}}$ and $\mathbf{n}_0$, unit vector characterizing the local orientation of the fiber.

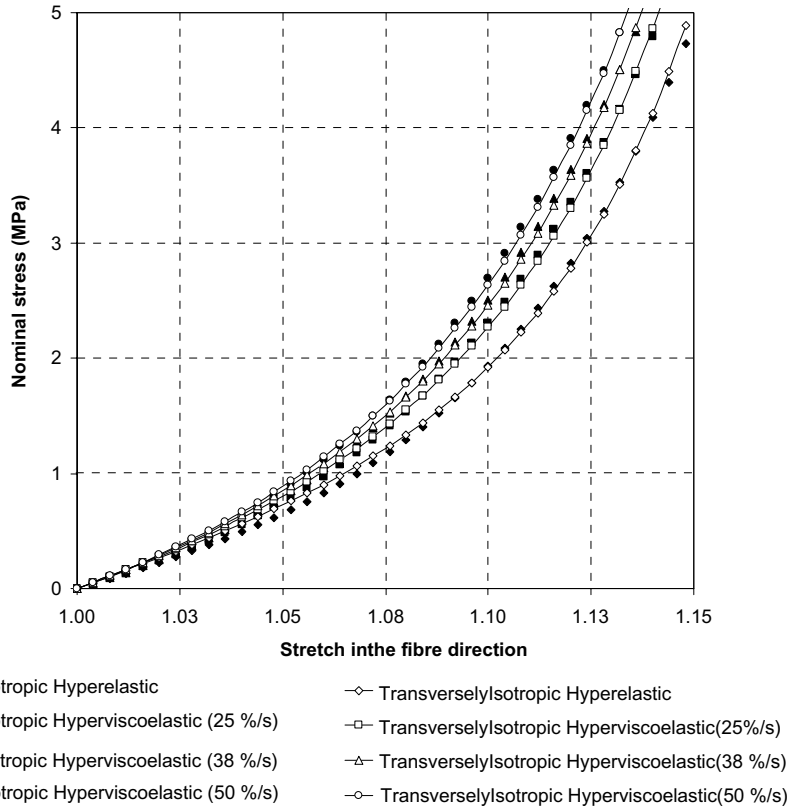

Fig. 2. Analytical stress-stretch curves obtained at four different elongation rates: 0.3, 6, 9 and 12 mm s^{-1} for the transversely isotropic hyperviscoelastic law by identification with the analytical curves from Pioletti's model. The loading scenario corresponds to *uniaxial extension along the fiber direction* (aligned with the direction $\mathbf{E}_3$). The nominal stress P_{33} which corresponds to the actual force divided by the initial cross section, is easily related to the second Piola–Kirchhoff stress tensor by $P_{33} = F_{33}S_{33}$ The curves representing the response of the transversely isotropic hyperviscoelastic law correspond to the material parameters from Table 2. It is noteworthy that the elongation rates 0.3, 6, 9 and 12 mm s^{-1} correspond respectively to the deformation rates 1.2% s^{-1}, 25% s^{-1}, 38% s^{-1} and 50% s^{-1}. For this loading scenario the deformation gradient is: $\mathbf{F} = \frac{1}{\sqrt{\lambda}}\mathbf{E}_1 \otimes \mathbf{E}_1 + \frac{1}{\sqrt{\lambda}}\mathbf{E}_2 \otimes \mathbf{E}_2 + \lambda \mathbf{E}_3 \otimes \mathbf{E}_3$.

Table 1
Material coefficients obtained by Pioletti et al. (1998) by identification of an isotropic viscohyperlastic potential with experimental tensile tests on human ACLs

Material coefficients	α [MPa]	β	η [MPa s]
Pioletti et al. (1998)	0.30 ± 0.08	12.20 ± 2.18	39.29 ± 10.98

The elastic response was assumed to be the response at the lowest strain rate (0.012% s^{-1}) while tensile tests at 25% s^{-1}, 38% s^{-1} and 50% s^{-1} allowed the determination of the viscosity coefficient η.

4.2. Elastic contribution to the Helmholtz free energy function ψ

The purely elastic behavior of the tissue, represented by the function ψ^e, is assumed to arise from the mechanical response of the ground substance and the collagen fibers. Because of the high water content of soft connective tissues, the biological material is assumed to be incompressible. As a direct consequence, the

Table 2
Material coefficients obtained by identification of the present transversely isotropic viscohyperelastic model with the Pioletti's model (Pioletti et al., 1998)

c_1 [MPa]	c_2 [MPa]	c_3	η_1 [MPa s]	η_2 [MPa s]
1 ± 0.2629	1.7939 ± 0.2859	11.2055 ± 1.1424	0.0523 ± 3.2654	15.0087 ± 2.5053

During the non-linear optimization procedure the following constraint was enforced: $c_1 = 1$. The correlation coefficient was $R^2 = \{0.99361105\}$.

third invariant of $\mathbf{C}$, I_3, is equal to 1 and does not appear in the equations. Therefore ψ^e is reduced to $\psi^e(I_1, I_4)$. In the absence of relevant experimental data, the interactions between the fibers and the matrix, that would be represented by a function coupling I_1 and I_4, are not accounted for. In consequence $\psi^e(I_1, I_4)$ is split into the sum of a strain energy function representing the elastic contribution of the ground substance ψ^e_m and a strain energy function encompassing the anisotropic behaviour introduced by the collagen fibers ψ^e_f (Spencer, 1992)

$$\psi^e = \psi^e(I_1, I_4) = \psi^e_m(I_1) + \psi^e_f(I_4) \tag{60}$$

This hypothesis has been used successfully by numerous researchers to describe the mechanical behavior of soft tissues (Hirokawa and Tsuruno, 2000; Holzapfel et al., 1996; Humphrey, 1990; Humphrey and Yin, 1987; Limbert, 2001; Limbert et al., 2004; Limbert and Taylor, 2001a; Puso and Weiss, 1998; Weiss et al., 1996).

ψ^e_m is chosen as being the strain energy function of an incompressible neo-Hookean material (Ogden, 1984):

$$\psi^e_m = c_1(I_1 - 3) \tag{61}$$

The neo-Hookean model has been used by several investigators to represent the elastic behavior of the ground substance of connective tissues (Limbert, 2001; Limbert et al., 2004; Limbert and Taylor, 2001a; Weiss et al., 1995; Weiss et al., 1996). For an incompressible material, ψ^e_m also exhibits the important property of convexity which assures stability of the material.

The typical non-linear stiffening of biological soft connective tissues under tension is provided by the progressive recruitment of the collagen fibers. An exponential form is suitable to represent this behavior (Eq. (62)-2). Collagen fibers do not support significant compressive loads and collagenous structures are prone to buckle under very small compressive forces (Eq. (62)-1). The mechanical response of ligaments under tension along the collagen fibers is only stiffening up to a certain value of strain, typically 2–3% (Carlstedt and Nordin, 1989). After that point, the tensile behavior of the composite fibrous structure is almost linear until failure (Eq. (62)-3).

Based on these observations, the following convex function of I_4 is proposed to represent the mechanical contribution of the fibers:

$$\psi^e_f = g(I_4) = \begin{cases} 0 & \text{if } I_4 \leqslant 1 \\ \dfrac{c_3}{2c_4}\left[e^{c_4(I_4-1)^2} - 1\right] & \text{if } I_4 \leqslant I_4^* \\ c_5\sqrt{I_4} + c_6 \ln I_4 & \text{if } I_4 \geqslant I_4^* \end{cases} \tag{62}$$

c_1, c_2, c_3, c_4, c_5, c_6 and I_4^* are material parameters. c_6 is determined by postulating C^1-continuity of $g(I_4)$ at $I_4 = I_4^*$ where $I_4^* = (\lambda^*)^2$, λ^* being the stretch at which collagen fibers are uncrimped.

The objective of the present development was to fit the constitutive parameters of the particular Helmholtz free energy function ψ with the experimental data collected by Pioletti (Pioletti, 1997; Pioletti

et al., 1998) for the human anterior cruciate ligament. These authors used an exponential form for the isotropic strain energy function based on the form proposed by Veronda and Westmann (1970).

This form was found to fit very well the experimental data up to a value of stretch of 1.12 along the collagen fiber direction (Pioletti, 1997; Pioletti et al., 1998).

Given that Pioletti et al. (Pioletti, 1997; Pioletti et al., 1998) did not determine I_4^* experimentally and given that the exponential function was found suitable to represent the mechanical response of the ACL up to a stretch of 1.1–1.125, that is, beyond the usual toe region, it was decided to eliminate the linear term from the stress response $I_4 \frac{\mathrm{d}(c_5\sqrt{I_4}+c_6 \ln I_4)}{\mathrm{d}I_4} = c_5\sqrt{I_4} + c_6 = c_5\lambda + c_6$ and reduce $\psi_{\mathrm{f}}^{\mathrm{e}}$ to the following form:

$$\psi_{\mathrm{f}}^{\mathrm{e}} = g(I_4) = \begin{cases} 0 & \text{if } I_4 \leqslant 1 \\ \dfrac{c_2}{2c_3}[e^{c_3(I_4-1)^2} - 1] & \text{if } I_4 > 1 \end{cases} \tag{63}$$

c_1, c_2 and c_3 are material parameters which warrant convexity of the elastic potentials provided that they are all positive.

4.3. Viscous contribution to the Helmholtz free energy function ψ

The viscous response of the material is assumed to be provided by the ground substance and from the collagen fibers. In the absence of experimental data, it is hypothesized that matrix and fiber viscous contributions are additive. This is a simplifying assumption that is believed to provide a good compromise between analytical–experimental tractability and accuracy. It is important to remind that the present developments were aimed at the development of a *phenomenological* model capable of describing the *macroscopic* behavior of soft connective tissues. The important characteristic of phenomenological models is that they do not necessarily reflect the microscopic structure of the material and its behavior at the microscopic scale. Moreover, the viscous response of the tissue is augmented by a term which arises only when the collagen fibers start to extend (Eq. (64)-2). This captures the viscous interactions between the ground substance and the collagen fibers after uncrimping. The following viscosity function ψ^{v} is therefore proposed:

$$\psi^{\mathrm{v}} = \psi(J_2, I_1, J_5, I_4,) = \begin{cases} \eta_1 J_2(I_1 - 3) & \text{if } I_4 \leqslant 1 \\ \eta_1 J_2(I_1 - 3) + \dfrac{1}{2}\eta_2 J_5(I_4 - 1)^2 & \text{if } I_4 > 1 \end{cases} \tag{64}$$

η_1 and η_2 are material parameters which warrant convexity of the viscous potentials ψ^{v}, provided that they are all positive.

Again, by incorporating elastic invariants (I_1 and I_4) in the viscous potential ψ^{v}, one accounts for coupling between elastic and viscous effects.

4.4. Second Piola–Kirchhoff elastic stress tensor

As a reaction to the kinematic constraint of incompressibility ($I_3 = 1$), an arbitrary pressure p enters the stress under the form of a Lagrangean multiplier, determined only by the equations of equilibrium or motion and the boundary conditions (not the constitutive equations).

By combining Eqs. (33), (61) and (63), the second Piola–Kirchhoff elastic stress tensor is obtained as

$$\mathbf{S}^{\mathrm{e}} = \begin{cases} 2c_1\mathbf{1} + p\mathbf{C}^{-1} & \text{if } I_4 \leqslant 1 \\ 2[c_1\mathbf{1} + c_2 e^{c_3(I_4-1)^2}(I_4 - 1)\mathbf{N}_0] + p\mathbf{C}^{-1} & \text{if } I_4 > 1 \end{cases} \tag{65}$$

4.5. Second Piola–Kirchhoff viscous stress tensor

By combining Eqs. (34) and (64), the second Piola–Kirchhoff viscous stress tensor is obtained as:

$$\mathbf{S}^{\mathrm{v}} = \begin{cases} 2[\eta_1(I_1-3)\dot{\mathbf{C}}] & \text{if } I_4 \leqslant 1 \\ 2\left[\eta_1(I_1-3)\dot{\mathbf{C}} + \frac{1}{2}\eta_2(I_4-1)^2 \boldsymbol{\Upsilon}_{\mathbf{n}_0\dot{\mathbf{C}}}\right] & \text{if } I_4 > 1 \end{cases} \tag{66}$$

4.6. Identification of material parameters

In order to identify the proposed transversely isotropic hyperviscoelastic constitutive law with experimental data related to tensile tests (in the natural fiber orientation) of the human anterior cruciate ligament (Pioletti et al., 1998), explicit analytical expressions of the stress in the fiber direction are necessary.

4.6.1. Uniaxial extension in the fiber direction

As for the experimental and identification tests performed by Pioletti et al. (1998), it is assumed a state of homogeneous deformation with isochoric kinematics. The stretch in the direction of the fibers is noted λ. If the fiber direction is aligned with the direction $\mathbf{E}_3$ in the reference configuration, the deformation gradient is given by $\mathbf{F} = \frac{1}{\sqrt{\lambda}}(\mathbf{E}_1 \otimes \mathbf{E}_1 + \mathbf{E}_2 \otimes \mathbf{E}_2) + \lambda \mathbf{E}_3 \otimes \mathbf{E}_3$. The derivative of J_5 is $\frac{\partial J_5}{\partial \dot{\mathbf{C}}} = 2\dot{C}_{33}\mathbf{n}_0 \otimes \mathbf{n}_0 = 2\dot{C}_{33}\mathbf{E}_3 \otimes \mathbf{E}_3$.

In this particular configuration, the non-null component of the elastic second Piola–Kirchhoff stress tensor is:

$$S^{\mathrm{e}}_{33} = \begin{cases} 2c_1\left(1 - \frac{1}{\lambda^3}\right) & \text{if } \lambda \leqslant 1 \\ 2c_1\left(1 - \frac{1}{\lambda^3}\right) + 2c_2 \mathrm{e}^{c_3(\lambda^2-1)^2}(\lambda^2 - 1) & \text{if } \lambda > 1 \end{cases} \tag{67}$$

The non-null component of the viscous second Piola–Kirchhoff stress tensor is

$$S^{\mathrm{v}}_{33} = \begin{cases} 2\eta_1\left(\lambda^2 + \frac{2}{\lambda} - 3\right)\left(-\frac{\dot{C}_{11}}{\lambda^3} + \dot{C}_{33}\right) & \text{if } \lambda \leqslant 1 \\ 2\eta_1\left(\lambda^2 + \frac{2}{\lambda} - 3\right)\left(-\frac{\dot{C}_{11}}{\lambda^3} + \dot{C}_{33}\right) + 2\eta_2(\lambda^2-1)^2\dot{C}_{33} & \text{if } \lambda > 1 \end{cases} \tag{68}$$

Because of the incompressibility constraint the principal strain rates are dependent upon the following relation:

$$\dot{C}_{11} = -\frac{2\dot{C}_{33}}{(C_{33})^3} = -\frac{2\dot{C}_{22}}{(C_{22})^3} \tag{69}$$

which leads to

$$S^{\mathrm{v}}_{33} = \begin{cases} 2\eta_1\left(\lambda^2 + \frac{2}{\lambda} - 3\right)\left(1 + \frac{1}{2\lambda^6}\right)\dot{C}_{33} & \text{if } \lambda \leqslant 1 \\ 2\eta_1\left(\lambda^2 + \frac{2}{\lambda} - 3\right)\left(1 + \frac{1}{2\lambda^6}\right)\dot{C}_{33} + 2\eta_2(\lambda^2-1)^2\dot{C}_{33} & \text{if } \lambda > 1 \end{cases} \tag{70}$$

The isotropic viscohyperelastic potential proposed by Pioletti et al. (1998) is the following:

$$\psi = \psi(I_1, I_2, J_2) = \alpha e^{\beta(I_1-3)} - \frac{\alpha\beta}{2}(I_2 - 3) + \frac{\eta}{4}J_2(I_1 - 3) \tag{71}$$

where α, β and η are material parameters consigned in Table 1.

The non-null component of the elastic second Piola–Kirchhoff stress tensor for Pioletti's model is

$$S_{33}^{e} = \alpha\beta\left[\frac{-2e^{\beta\left(\lambda^2+\frac{2}{\lambda}-3\right)}}{\lambda^3} + \frac{1}{\lambda} + \frac{1}{\lambda^4} + 2e^{\beta\left(\lambda^2+\frac{2}{\lambda}-3\right)} - \frac{2}{\lambda}\right] \tag{72}$$

The non-null component of the viscous second Piola–Kirchhoff stress tensor for Pioletti's model is

$$S_{33}^{v} = \eta\dot{\lambda}\left(\lambda^2 + \frac{2}{\lambda} - 3\right)\left(1 + \frac{1}{2\lambda^6}\right) \tag{73}$$

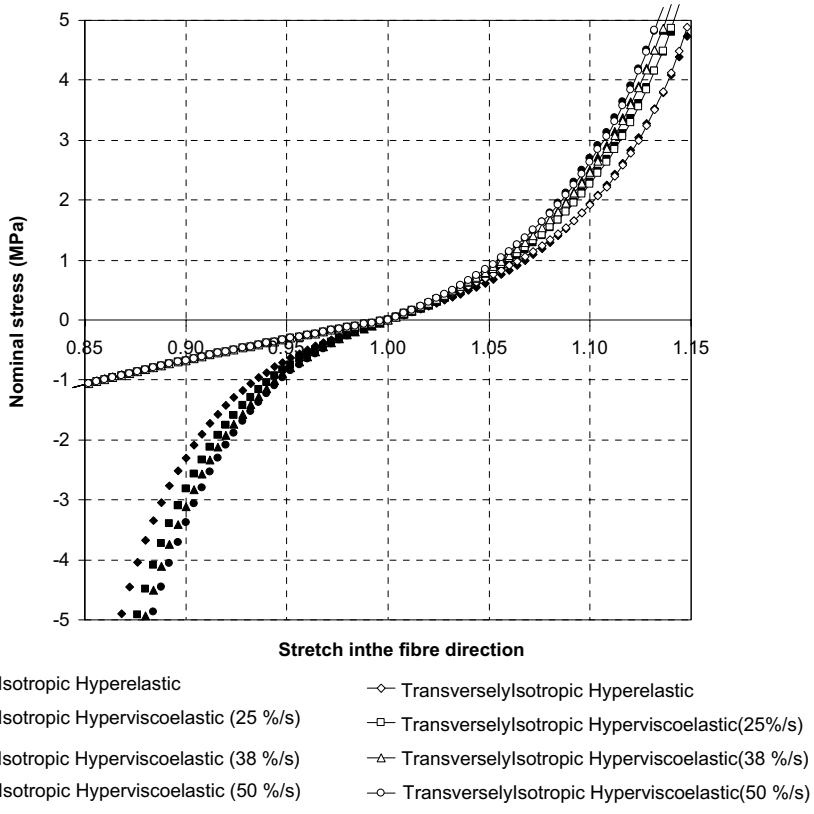

Fig. 3. Comparison between the present transversely isotropic hyperviscoelastic model and Pioletti's isotropic hyperviscoelastic model. Stress-stretch curves obtained at four different elongation rates: 0.3, 6, 9 and 12 mm s^{-1}. The loading scenario corresponds to *uniaxial compression–extension* along the fiber direction (aligned with the direction $\mathbf{E}_3$). The curves representing the response of the transversely isotropic hyperviscoelastic law correspond to material parameters from Table 2. It is noteworthy that the elongation rates 0.3, 6, 9 and 12 mm s^{-1} correspond, respectively, to the deformation rates 1.2% s^{-1}, 25% s^{-1}, 38% s^{-1} and 50% s^{-1}. The isotropic hyperviscoelastic model exhibits an unrealistically high stiffness in compression along the fiber direction whilst the transversely isotropic model overcomes this unwanted feature. For this loading scenario the deformation gradient is: $\mathbf{F} = \frac{1}{\sqrt{\lambda}}\mathbf{E}_1 \otimes \mathbf{E}_1 + \frac{1}{\sqrt{\lambda}}\mathbf{E}_2 \otimes \mathbf{E}_2 + \lambda\mathbf{E}_3 \otimes \mathbf{E}_3$.

The global response of the material is given by $S_{33} = S^{e}_{33} + S^{v}_{33}$. Using a least-square non-linear optimization procedure, the material parameters c_1, c_2, c_3, η_1 and η_2 were determined from the analytical curves, previously identified by Pioletti et al. (1998). As these curves were obtained for tensile tests in the fiber direction and by assuming isotropy of the material, it was necessary to relate the response of the matrix when no fiber contributes. This was done by giving the estimated value of 1 MPa to the compliant solid matrix, also called ground substance (Ault and Hoffman, 1992; Limbert, 2001; Limbert et al., 2004; Limbert and Taylor, 2001a). The graphic results of the identification is represented in Fig. 2. After identification of the transversely isotropic hyperviscoelastic potential with Pioletti's data and to check the performance of the model in other simple loading situations, equibiaxial compression–extension along the fiber and isotropy direction, strip biaxial compression extension along the fiber direction and pure shear in the isotropy plane were simulated (Figs. 4–9). Deformations are assumed to be homogeneous.

5. Results and discussion

During the identification procedure it was found that values of η_1 greater than 0.055 MPa s^{-1} led to unphysical behavior for high strain rates (50% s^{-1}) in the case of equibiaxial compression–extension along

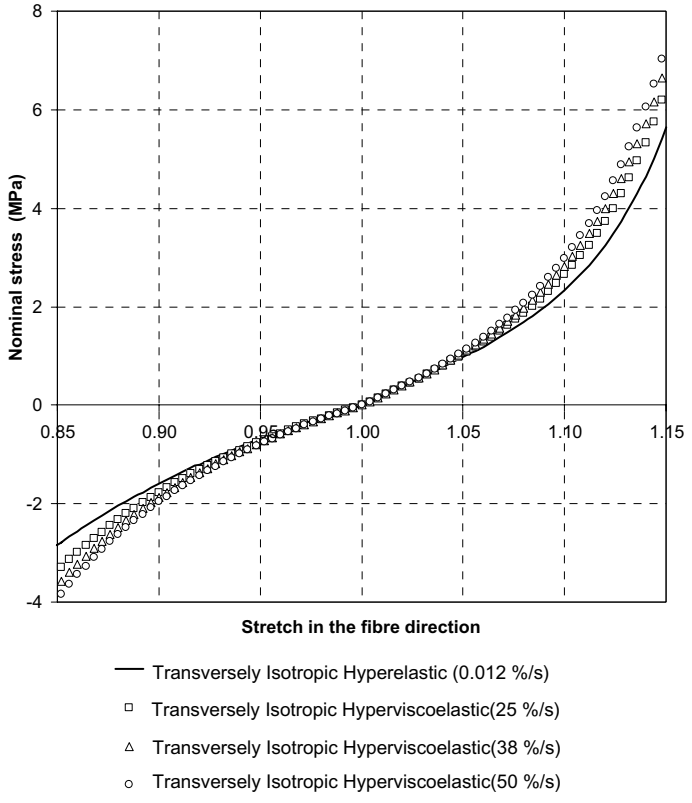

Fig. 4. Analytical stress-stretch curves (nominal stress P_{33} along the direction $\mathbf{E}_3$) obtained at four different elongation rates: 0.3, 6, 9 and 12 mm s^{-1} for the present isotropic hyperviscoelastic model. The loading scenario corresponds to *equibiaxial compression–extension* along the fiber direction (aligned with the direction $\mathbf{E}_3$) and along the axis aligned with $\mathbf{E}_2$. Material parameters of the transversely isotropic hyperviscoelastic law are taken from Table 2. For this loading scenario the deformation gradient is: $\mathbf{F} = \frac{1}{\lambda^2}\mathbf{E}_1 \otimes \mathbf{E}_1 + \lambda \mathbf{E}_2 \otimes \mathbf{E}_2 + \lambda \mathbf{E}_3 \otimes \mathbf{E}_3$.

the fiber direction and along any axis perpendicular to it. Examples of this were positive stresses in compression and negative in tension for certain ranges of stretch. Based on this finding, Pioletti's model was checked for this particular loading scenarios and unphysical behavior was also observed, especially since the viscosity coefficient η has a value of 39.29 MPa. This highlights the importance of testing a model for different loading scenarios and for various strain and strain rate ranges. It is also relevant to keep in mind that homogeneous deformation loading scenarios are highly idealized cases that are likely not to be encountered in real-life problems. Further efforts should be directed towards exploring new functional form for the elastic and viscous potentials as well as studying the mathematical properties of the associated elasticity and viscosity tensors which can lead to the establishment of explicit constitutive restrictions.

The proposed Helmoltz free energy function, while encompassing essential features of the ligaments (non-linear behaviour, stiffening in the fiber direction, high compliance in compression along the fiber direction, incompressibility, finite strain, anisotropic viscous response and strain rate effects), was capable of fitting accurately the analytical–experimental curves from Pioletti et al. (1998).

The strain rate effects, observed by Pioletti et al. (1998), are therefore also highlighted by the new constitutive model (Figs. 2 and 3). The elastic response is described by only three parameters while the viscous response is described by two parameters.

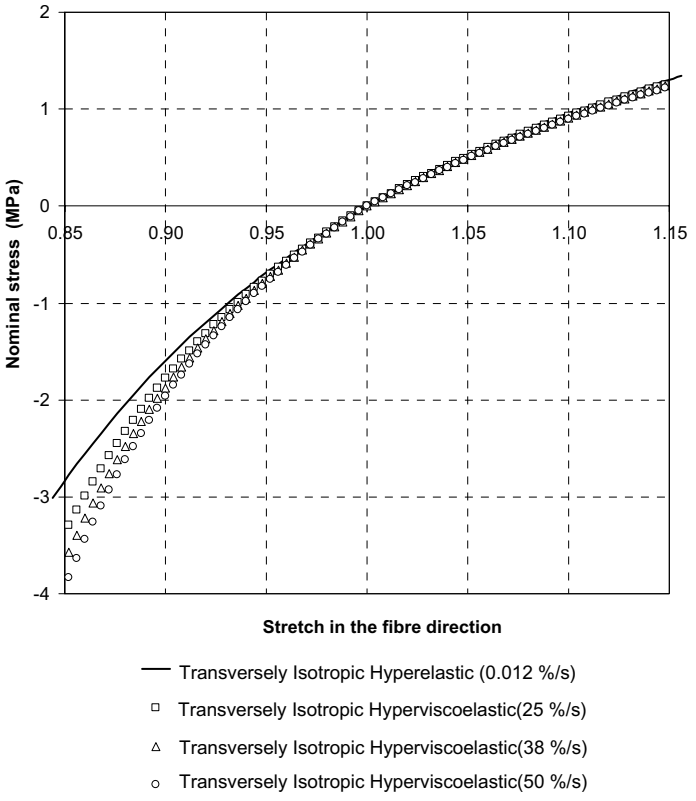

Fig. 5. Analytical stress-stretch curves (nominal stress P_{22} along the direction $\mathbf{E}_2$) obtained at four different elongation rates: 0.3, 6, 9 and 12 mm s^{-1} for the present isotropic hyperviscoelastic model. The loading scenario corresponds to *equibiaxial compression–extension* along the fiber direction (aligned with the direction $\mathbf{E}_3$) and along the axis aligned with $\mathbf{E}_2$. Material parameters of the transversely isotropic hyperviscoelastic law are taken from Table 2. For this loading scenario the deformation gradient is: $\mathbf{F} = \frac{1}{\lambda^2}\mathbf{E}_1 \otimes \mathbf{E}_1 + \lambda \mathbf{E}_2 \otimes \mathbf{E}_2 + \lambda \mathbf{E}_3 \otimes \mathbf{E}_3$.

In the optimization procedure, in order to fit experimental data from Pioletti et al. (1998), the constitutive requirement put on the small value of the isotropic viscosity coefficient η_1 (to prevent introduction of unphysical behaviors) has led to a dominant influence of the anisotropic viscosity coefficient η_2 on the viscous response of the transversely isotropic hyperelastic material in uniaxial extension along the fiber direction. This has the effect of attenuating the viscous effects when the material undergoes uniaxial compression. On Fig. 3 one can observe that the viscohyperelastic responses at the various strain rates (0.012 (purely elastic case), 25% s^{-1}, 38% s^{-1} and 50% s^{-1}) are nearly identical. This is also observed for the strip biaxial compression case (Figs. 6 and 7).

The basic hypothesis to justify the extension of Pioletti's model to the transverse isotropy case was that isotropic models perform badly when subjected to compression along the natural fiber orientation. In fact, high unphysiological compressive stresses are generated and this is clearly apparent in Fig. 3. Unlike the nearly symmetrical response in tension and compression along the fibers, observed for the isotropic model, the transversely isotropic model exhibits a much softer response in compression. This is a clear improvement over isotropic models and shows how particular structural features can be incorporated into phenomenological constitutive equations.

Figs. 4 and 5 presents the response of the material submitted to equibiaxial compression-extension. As expected from the constitutive formulation, the response in compression and extension is identical along the fiber direction and along the principal direction in the plane of isotropy ($\mathbf{E}_2$). As for the uniaxial extension

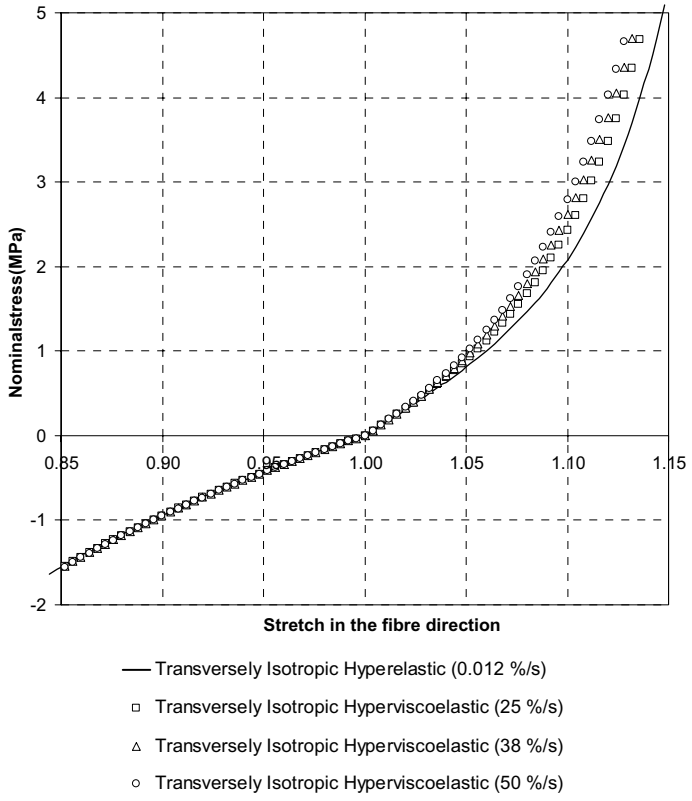

Fig. 6. Analytical stress-stretch curves (nominal stress P_{33} along the direction $\mathbf{E}_3$) obtained at four different elongation rates: 0.3, 6, 9 and 12 mm s^{-1} for the present isotropic hyperviscoelastic model. The loading scenario corresponds to *strip biaxial compression–extension along the fiber direction* (aligned with the direction $\mathbf{E}_3$). Material parameters of the transversely isotropic hyperviscoelastic law are taken from Table 2. For this loading scenario the deformation gradient is: $\mathbf{F} = \frac{1}{\lambda}\mathbf{E}_1 \otimes \mathbf{E}_1 + \mathbf{E}_2 \otimes \mathbf{E}_2 + \lambda \mathbf{E}_3 \otimes \mathbf{E}_3$.

along the fiber direction, the strain rate effects can also be observed. In extension along the axes $\mathbf{E}_2$, the viscoelastic response is lower in magnitude than the purely hyperelastic response. This effect is explained by the fact that the simultaneous extension along $\mathbf{E}_3$, has dominant viscous effects (dependence on the anisotropic viscosity coefficient η_2) on the resulting hydrostatic pressure equilibrating the extension along $\mathbf{E}_2$.

Figs. 6 and 7 present the response of the material submitted to strip biaxial compression–extension along the fiber direction. In compression, the response is stiffer along the fiber than along $\mathbf{E}_2$. Strain rates effects are apparent in extension along the fiber direction (Fig. 6).

Figs. 8 and 9 present the response (respectively, P_{12} and P_{21}) of the material submitted to pure shear in the plane of isotropy. It is worthy to note that the nominal stress tensor is not symmetric. Viscous effects are clearly dominant with respect to the elastic response and the shapes of the stress-stretch curves is closely related to the strain rates at which the shear tests are performed.

The hyperelastic response of the ground substance was assumed to be governed by a neo-Hookean strain energy function. Although this hypothesis is suitable to represent the isotropic mechanical response of the tissue it is believed that alternative strain energy functions must be investigated as recently proposed by Weiss et al. (2002). Similarly, other forms of strain energy functions for the fiber contributions should be considered.

As an alternative approach to the present study, the work by Hoffman and Grigg (2002) (and references given therein) presents other possible ways to investigate experimentally the mechanical response of soft

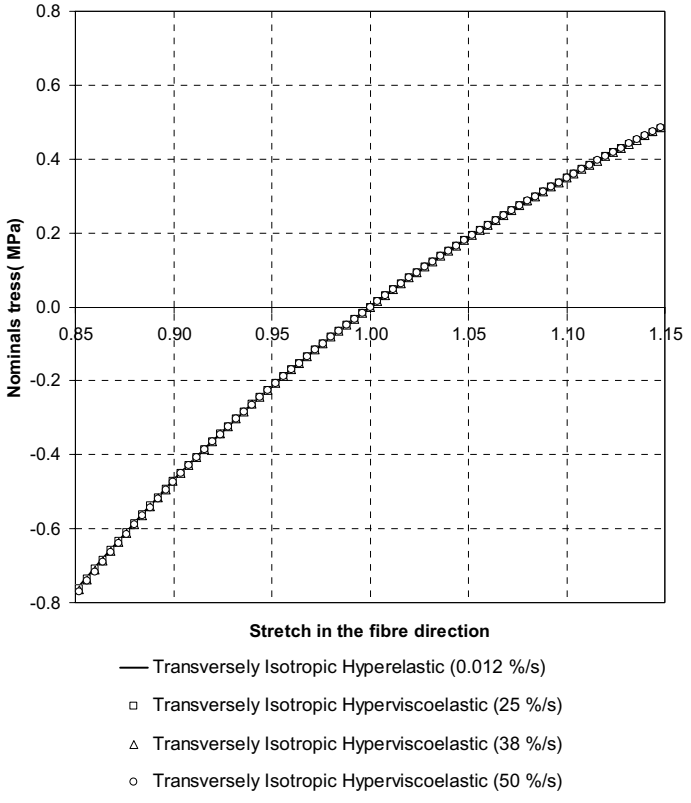

Fig. 7. Analytical stress-stretch curves (nominal stress P_{22} along the direction $\mathbf{E}_2$) obtained at four different elongation rates: 0.3, 6, 9 and 12 mm s^{-1} for the present isotropic hyperviscoelastic model. The loading scenario corresponds to *strip biaxial compression–extension along the fiber direction* (aligned with the direction $\mathbf{E}_3$). Material parameters of the transversely isotropic hyperviscoelastic law are taken from Table 2. For this loading scenario the deformation gradient is: $\mathbf{F} = \frac{1}{\lambda}\mathbf{E}_1 \otimes \mathbf{E}_1 + \mathbf{E}_2 \otimes \mathbf{E}_2 + \lambda \mathbf{E}_3 \otimes \mathbf{E}_3$.

tissues. The idea is to apply a pseudorandom Gaussian stress input to the tissue to be tested and to measure the strain response. From the output, the Volterra–Wiener kernels are calculated. The advantage of this protocol is that no a priori forms of the constitutive equations are required and that the pseudorandom stress input does not restrict the testing to specific loading scenarios. In consequence, the calculated material parameters are more likely to encompass a larger domain of validity frequency wise. In their study, Hoffman and Grigg (2002) considered only uniaxial testing on rat skin and medial collateral ligament although the method can be applied to multi-axial testing. Moreover, this experimental approach can accommodate linear as well as non-linear viscoelastic effects and can distinguish their respective influence of the tissue behaviour. A possible drawback is the practical testing of specimens for large deformations and for extremely short times.

Comparable work has been performed by Quaglini et al. (2002). The authors used a discrete-time non-linear Wiener model for determining the relaxation characteristics of bovine pericardium. Like in the study of Hoffman and Grigg (2002), it was found that the non-linear kernel is necessary to capture more accurately the mechanical response of the tissue. This approach is also suitable for implementation into a predictive numerical code.

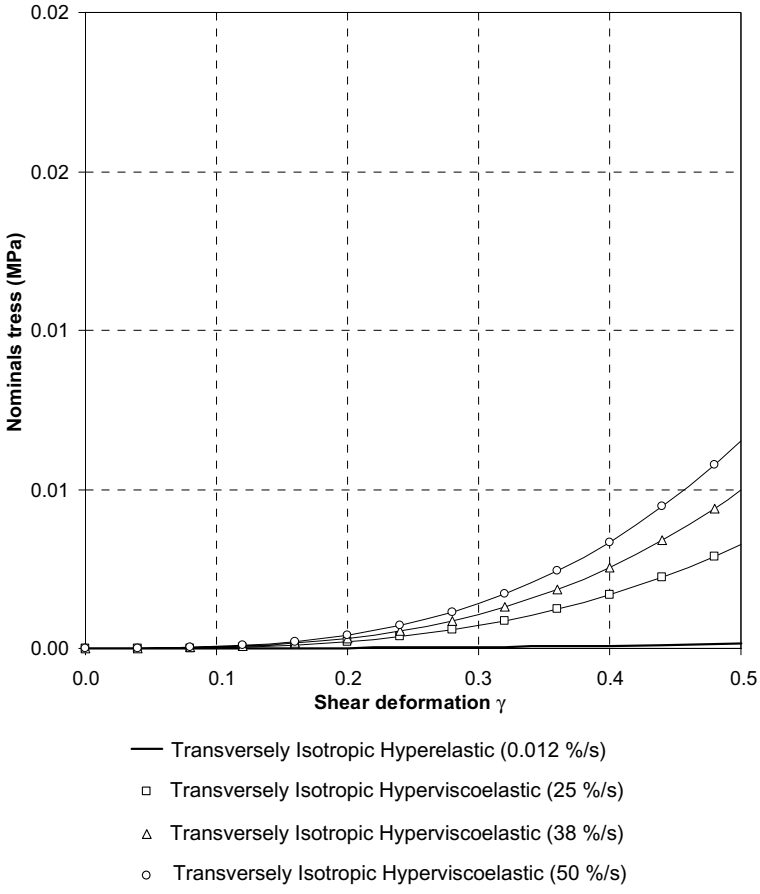

Fig. 8. Analytical stress-stretch curves (nominal shear stress P_{12}) obtained at four different elongation rates: 0.3, 6, 9 and 12 mm s^{-1} for the present isotropic hyperviscoelastic model. The loading scenario corresponds to *pure shear in the plane of isotropy* (defined by $\mathbf{E}_1$ and $\mathbf{E}_2$). Material parameters of the transversely isotropic hyperviscoelastic law are taken from Table 2. For this loading scenario the deformation gradient is: $\mathbf{F} = \gamma \mathbf{E}_1 \otimes \mathbf{E}_2 + \mathbf{E}_1 \otimes \mathbf{E}_1 + \mathbf{E}_2 \otimes \mathbf{E}_2 + \mathbf{E}_3 \otimes \mathbf{E}_3$.

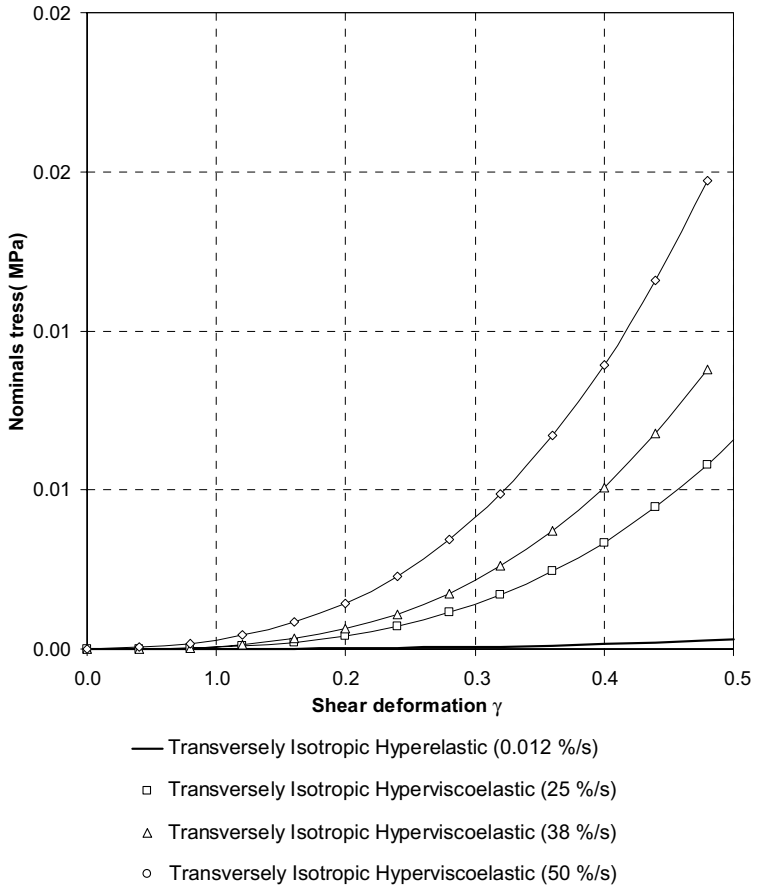

Fig. 9. Analytical stress-stretch curves (nominal shear stress P_{21}) obtained at four different elongation rates: 0.3, 6, 9 and 12 mm s^{-1} for the present isotropic hyperviscoelastic model. The loading scenario corresponds to *pure shear in the plane of isotropy* (defined by $\mathbf{E}_1$ and $\mathbf{E}_2$). Material parameters of the transversely isotropic hyperviscoelastic law are taken from Table 2. For this loading scenario the deformation gradient is: $\mathbf{F} = \gamma \mathbf{E}_1 \otimes \mathbf{E}_2 + \mathbf{E}_1 \otimes \mathbf{E}_1 + \mathbf{E}_2 \otimes \mathbf{E}_2 + \mathbf{E}_3 \otimes \mathbf{E}_3$.

The particular Helmholtz free energy function described in Section 4 is such that the viscous stress tensor depends linearly on the rate of deformation although the general framework developed in Section 3 can accommodate a second-order non-linear dependence. The Helmholtz free energy function chosen was a simple application of the constitutive framework and was limited by the nature of the experimental data collected by Pioletti et al. (1998) which were identified with a linear strain rate model.

It is believed that in the context of high strain rate loading situations subjecting ligaments, the inclusion of non-linear rate terms is relevant but not necessarily in the case of uniaxial tensile tests performed at constant strain rates. Additional studies will be required to answer these questions with certainty.

6. Concluding remarks

In this study, the constitutive framework of Noll (1958), previously applied to soft tissue modeling by Pioletti et al. (1998), has been developed for the specific case of transverse isotropy at the finite strain

regime. The continuum constitutive model developed by Pioletti et al. (1998) had the merit to encompass strain rate effects by using the rate of deformation as an explicit variable. However, a limitation of this constitutive law was the assumption of isotropy. In fact, due to their fibrous structure (collagen fibers embedded in a highly compliant solid matrix), modeling ligaments as anisotropic structures is indeed a basic necessary requirement (Limbert, 2001; Limbert and Taylor, 2001a; Limbert and Taylor, 2001b; Limbert and Taylor, 2002). Although viscohyperelastic constitutive laws featuring transverse isotropy were already available (Holzapfel, 2000; Puso and Weiss, 1998), none of them was describing faithfully the very short-term stiffening effect associated with strain rate, as observed in biological soft tissue mechanics (Woo et al., 1981). In order to circumvent this lack in the literature, a new constitutive framework was presented in the context of tensor formalism (with use of a structural tensor describing the local structural arrangement of the continuum) and thermodynamic potentials. The general constitutive law has been developed to take into account simultaneously the fibrous and viscous characteristics of biological soft tissues while remaining thermodynamically admissible (convexity of thermodynamic potentials enforced a priori).

New closed-form expressions of viscous stress tensors as well as fictitious viscosity tensors were derived in the general case of transverse isotropy, that is, without restricting the way (coupling) the invariants characterizing the viscosity appear in the expression of the viscous potential. The expression for the viscosity tensor is of interest, because, in addition of its relevance to predict and explore the mechanical behavior of a given material, this tensor holds fundamental mathematical properties of the constitutive law. Stability studies and constitutive restrictions generally rely on arguments based on these properties.

The general expressions of the stress, elasticity and viscosity tensors are also essential in the finite element implementation of constitutive laws for fiber-reinforced composites and it is hoped that they will be useful with this regards.

The present phenomenological formulation is fairly simple but its drawback lies in the fact that the tensorial invariants of the right Cauchy–Green deformation tensor, its rate and agencies of the structural tensor considered do not all have a physical interpretation. Applicability of the general viscohyperelastic fiber-reinforced composite model remains to be explored on experimental grounds but with suitable experimental material characterization one can envisage to integrate complex interactions between elemental constituents within a constitutive law.

This aspect is possibly the most challenging as well as separating and identifying viscous effects between the ground substance and the collagen fibers. In the present model it was assumed that the viscous response provided by the interactions between the collagen fibers and the ground substance was accounted only when the fibers are uncrimped. This possibly limits the applicability of the model for explicit accounting of the viscous interactions between the ground substance and the collagen fibers which are known to arise during uncrimping of the collagen fibers. Further studies should look at the way of integrating these characteristics into the constitutive equations and ways of designing appropriate experimental protocols to capture accurately elastic and viscous effects.

References

Almeida, E.S., Spilker, R.L., 1998. Finite element formulations for hyperelastic transversely isotropic biphasic soft tissues. Computer Methods in Applied Mechanics and Engineering 151, 513–538.

Ault, H.K., Hoffman, A.H., 1992. A composite micro-mechanical model for connective tissues: Part II—Application to rat tail tendon and joint capsule. Journal of Biomechanical Engineering 114, 142–146.

Boehler, J.P., 1978. Lois de comportement anisotrope des milieux continus. Journal de Mécanique 17, 153–190.

Boehler, J.P., 1987. Applications of tensor functions in solid mechanics. Springer, Wien.

Carlstedt, C.A., Nordin, M., 1989. Biomechanics of tendons and ligaments. In: Nordin, M., Frankel, V.H. (Eds.), Basic biomechanics of the musculoskeletal system. Lea & Febiger, Philadelphia, London.

Chiba, M., Komatsu, K., 1993. Mechanical responses of the periodontal ligament in the transverse section of the rat mandibular incisor at various velocities of loading in vitro. Journal of Biomechanics 26 (4/5), 561–570.
Cohen, H., Wang, C.C., 1987. On the response and symmetry of elastic materials with internal constraints. Archive of Rational Mechanics and Analysis 99, 1.
Coleman, B.D., Gurtin, M.E., 1967. Thermodynamics with internal state variables. Journal of Chemistry and Physics 47, 597–613.
Coleman, B.D., Noll, W., 1963. The thermodynamics of elastic materials with heat conduction and viscosity. Archive of Rational Mechanics and Analysis 13, 167–178.
Coleman, B.D., Noll, W., 1964. Material symmetry and thermostatic inequalities in finite elastic deformations. Archive of Rational Mechanics and Analysis 17, 87–111.
Ericksen, J.L., 1978. On the symmetry and stability of thermoelastic solids. Journal of Applied Mechanics 45, 740.
Ericksen, J.L., 1979. On the symmetry of deformable crystals. Archive of Rational Mechanics and Analysis 72, 1–13.
Ericksen, J.L., Rivlin, R.S., 1954. Large elastic deformations of homogeneous anisotropic materials. Journal of Rational Mechanics and Analysis 3, 281–301.
Fung, Y.C., 1973. Biorheology of soft tissues. Biorheology 10, 139–155.
Haut, R.C., 1983. Age-dependent influence of strain rate on the tensile failure of rat-tail tendon. Journal of Biomechanical Engineering 105, 296–299.
Haut, R.C., Little, R.W.A., 1972. A constitutive equation for collagen fibers. Journal of Biomechanics 5, 423–430.
Hirokawa, S., Tsuruno, R., 2000. Three-dimensional deformation and stress distribution in an analytical/computational model of the anterior cruciate ligament. Journal of Biomechanics 33, 1069–1077.
Hoffman, A.H., Grigg, P., 2002. Using uniaxial pseudorandom stress stimuli to develop soft tissue constitutive equations. Annals of Biomedical Engineering 30, 44–53.
Holzapfel, G.A., 2000. Nonlinear solid mechanics. A continuum approach for engineering. John Wiley & Sons, Chichester.
Holzapfel, G.A., Eberlein, R., Wriggers, P., Weizsäcker, H.W., 1996. Large strain analysis of soft biological membranes: Formulation and finite element analysis. Computer Methods in Applied Mechanics and Engineering 132, 45–61.
Humphrey, J.D., 1990. Determination of a constitutive relation for passive myocardium: I: A new functional form. Journal of Biomechanical Engineering 112, 333–339.
Humphrey, J.D., Yin, F.C.P., 1987. On constitutive relations and finite deformations of passive cardiac tissue: I: A pseudostrain energy function. Journal of Biomechanical Engineering 109, 298–304.
Kennedy, J.C., Hawkins, R.J., Willis, R.B., Danylchuck, K.D., 1976. Tension studies of human knee ligaments. Yield point, ultimate failure, and disruption of the cruciate and tibial collateral ligaments. Journal of Bone and Joint Surgery 58 A(3), 350–355.
Limbert, G., 2001. Finite element modelling of biological soft connective tissues. Application to the ligaments of the human knee. Ph.D. Thesis. School of Engineering Sciences, University of Southampton, UK.
Limbert, G., Taylor, M., 2001a. An explicit three-dimensional finite element model of an incompressible transversely isotropic hyperelastic material. Application to the study of the human anterior cruciate ligament. In: Bathe, K.J. (Ed.), First MIT Conference on Computational Fluid and Solid Mechanics, Cambridge, MA, USA, June 12–15. Elsevier Science, Amsterdam, pp. 319–322.
Limbert, G., Taylor, M., 2001b. Three-dimensional finite element modelling of the human anterior cruciate ligament. Influence of the initial stress field. In: Middleton, J., Jones, M.L., Pande, G.N. (Eds.), Computer Methods in Biomechanics and Biomedical Engineering, vol. 3. Gordon and Breach Science Publishers, London, pp. 355–360.
Limbert, G., Taylor, M., 2002. On the constitutive modeling of biological soft connective tissues. A general theoretical framework and tensors of elasticity for strongly anisotropic fiber-reinforced composites at finite strain. International Journal of Solids and Structures 398, 2343–2358.
Limbert, G., Middleton, J., Taylor, M., 2004. Finite element analysis of the human ACL subjected to passive anterior tibial loads. Computer Methods in Biomechanics and Biomedical Engineering 7 (1), 1–8.
Marsden, J.E., Hughes, T.J.R., 1994. Mathematical Foundations of Elasticity. Dover, New-York.
Negahban, M., Wineman, A.S., 1989a. Material symmetry and the evolution of anisotropies in a simple material—I. Change of reference configuration. International Journal of Nonlinear Mechanics 24, 521–536.
Negahban, M., Wineman, A.S., 1989b. Material symmetry and the evolution of anisotropies in a simple material – II. The evolution of material symmetry. International Journal of Nonlinear Mechanics 24, 537–549.
Noll, W., 1958. A mathematical theory of the mechanics of continuous media. Archive of Rational Mechanics and Analysis 2, 199–226.
Nowalk, M.D., Logan, S.E., 1991. Distinguishing biomechanical properties of intrinsinc and extrinsinc human wrist ligaments. Journal of Biomechanical Engineering 113, 85–93.
Ogden, R.W., 1984. Non-Linear Elastic Deformations. Ellis Horwood Ltd, West Sussex, England.
Pioletti, D.P., 1997. Viscoelastic properties of soft tissues: application to knee ligaments and tendons. Ph.D. Thesis. Département de Physique, Ecole Polytechnique Fédérale de Lausanne, Switzerland.

Pioletti, D.P., Rakotomanana, L.R., Benvenuti, J.F., Leyvraz, P.F., 1998. Viscoelastic constitutive law in large deformations: application to human knee ligaments and tendons. Journal of Biomechanics 31 (8), 753–757.

Puso, M.A., Weiss, J.A., 1998. Finite element implementation of anisotropic quasi-linear viscoelasticity using a discrete spectrum approximation. Journal of Biomechanical Engineering 1201, 62–70.

Quaglini, V., Previdi, F., Contro, R., Bittanti, S., 2002. A discrete-time nonlinear Wiener model for the relaxation of soft biological tissues. Medical Engineering and Physics 241, 9–19.

Spencer, A.J.M., 1992. Continuum theory of the mechanics of fibre-reinforced composites. Springer-Verlag, New York.

Ticker, J.B., Bigliani, L.U., Soslowsky, L.J., Pawluk, R.J., Flatow, E.L., Mow, V.C., 1996. Inferior glenohumeral ligament: geometric and strain-rate dependent properties. Journal of Shoulder and Elbow Surgery 5, 269–279.

Truesdell, C., Noll, W., 1992. The non-linear field theories of mechanics. Springer-Verlag, Berlin, New York.

Veronda, D.R., Westmann, R., 1970. Mechanical characterization of skin—finite deformations. Journal of Biomechanics 3, 111–124.

Weiss, J.A., Gardiner, J.C., Quapp, K.M., 1995. Material models for the study of soft tissue mechanics. In: International Conference on Pelvic and Lower Extremities Injuries, Washington, DC, December 4–6, pp. 249–261.

Weiss, J.A., Maker, B.N., Govindjee, S., 1996. Finite element implementation of incompressible transversely isotropic hyperelasticity. Computer Methods in Applied Mechanics and Engineering 135, 107–128.

Weiss, J.A., Gardiner, J.C., Bonifasi-Lista, C., 2002. Ligament material behavior is nonlinear, viscoelastic and rate-independent under shear loading. Journal of Biomechanics 357, 943–950.

Wineman, A.S., Pipkin, A.C., 1964. Material symmetry restrictions on constitutive equations. Archive of Rational Mechanics and Analysis 17, 184–214.

Woo, S.L.Y., Gomez, M.A., Akeson, W.H., 1981. The time and history-dependent viscoelastic properties of the canine medial collateral ligament. Journal of Biomechanical Engineering 103, 293–298.

Zheng, Q.S., Boehler, J.P., 1994. The description, classification, and reality of material and physical symmetries. Acta Mechanica 102, 73–89.